Report No. K-TRAN: KU-10-6 ▪ FINAL REPORT ▪ November 2011

Use of Flexible Facing for Soil Nail Walls

Sanat Pokharel, Ph.D.
Robert L. Parsons, Ph.D., P.E.
Jie Han, Ph.D., P.E.
Isaac Willems
The University of Kansas

Matthew Pierson, Ph.D.
Missouri State University

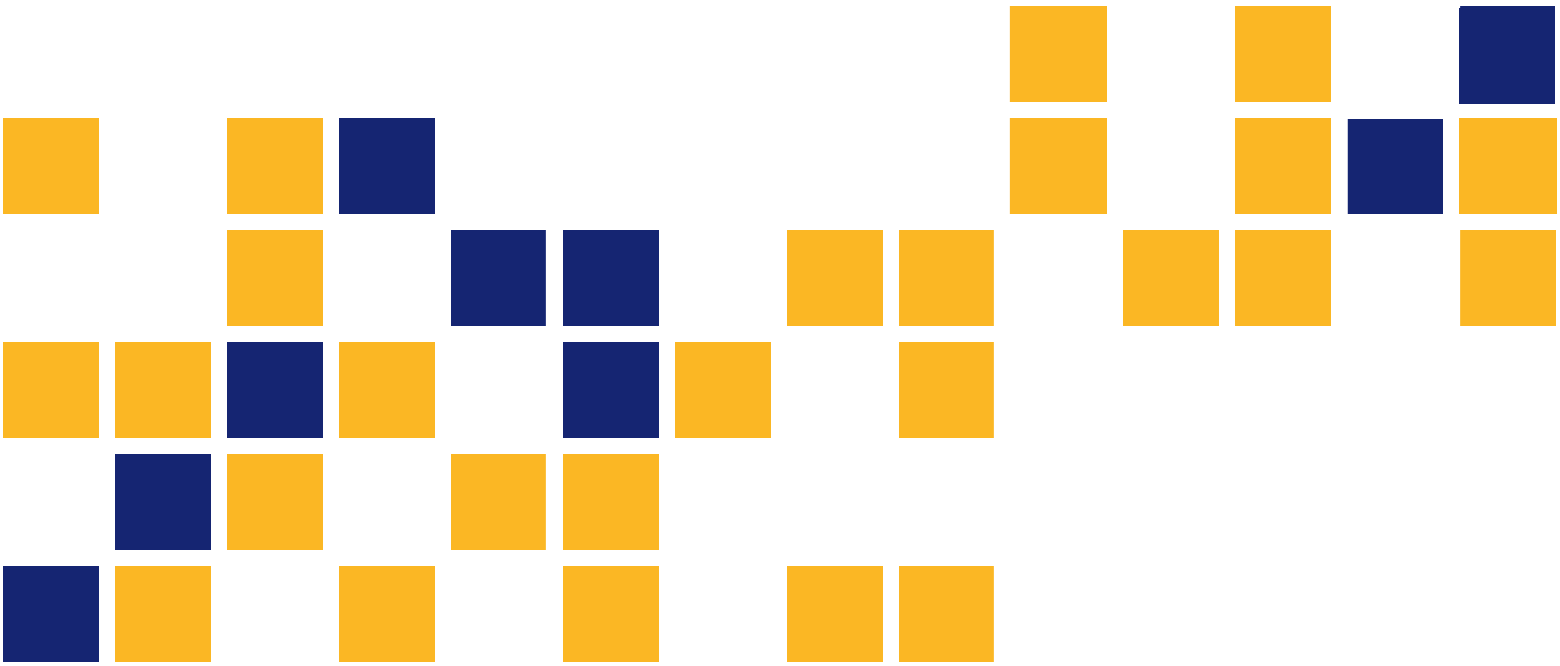

A cooperative transportation research program between
Kansas Department of Transportation,
Kansas State University Transportation Center, and
The University of Kansas

Kansas
Department of Transportation

1 Report No. K-TRAN: KU-10-6	**2 Government Accession No.**	**3 Recipient Catalog No.**
4 Title and Subtitle USE OF FLEXIBLE FACING FOR SOIL NAIL WALLS		**5 Report Date** November 2011 **6 Performing Organization Code**
7 Author(s) Sanat Pokharel, Ph.D.; Robert L. Parsons, Ph.D., P.E.; Matthew Pierson, Ph.D.; Jie Han, Ph.D., P.E.; Isaac Willems		**8 Performing Organization Report No.**
9 Performing Organization Name and Address University of Kansas Civil, Environmental & Architectural Engineering Department 1530 West 15th Street Lawrence, Kansas 66045-7609		**10 Work Unit No. (TRAIS)** **11 Contract or Grant No.** C1835
12 Sponsoring Agency Name and Address Kansas Department of Transportation Bureau of Materials and Research 700 SW Harrison Street Topeka, Kansas 66603-3745		**13 Type of Report and Period Covered** Final Report September 2009–February 2011 **14 Sponsoring Agency Code** RE-0535-01
15 Supplementary Notes For more information write to address in block 9.		

16 Abstract

Soil nail walls are a widely used technology for retaining vertical and nearly vertical cuts in soil. A significant portion of the cost of soil nail wall construction is related to the construction of a reinforced concrete face. The potential for use of a flexible facing design for soil nail walls to replace reinforced concrete facing was evaluated using three-dimensional finite difference modeling and physical testing of a 1.5 meter by 1.5 meter unit cell of a soil nail wall in clay. A steel mesh form of flexible facing was used as a substitute for concrete. The finite difference model predicted large vertical and horizontal deformations for surcharges of approximately 5 psi. In the physical testing, the flexible facing products performed well with regard to strength, but the facing experienced large vertical and horizontal deformations that were consistent with the numerical modeling. Based on these results, it is recommended that use of flexible facing as a substitute for reinforced concrete be limited to non-critical structures where large vertical and horizontal deformations are acceptable.

17 Key Words Soil nail walls, flexible facing		**18 Distribution Statement** No restrictions. This document is available to the public through the National Technical Information Service, Springfield, Virginia 22161	
19 Security Classification (of this report) Unclassified	**20 Security Classification (of this page)** Unclassified	**21 No. of pages** 70	**22 Price**

Form DOT F 1700.7 (8-72)

Use of Flexible Facing for Soil Nail Walls

Final Report

Prepared by

Sanat Pokharel, Ph.D.
Robert L. Parsons, Ph.D., P.E.
Jie Han, Ph.D., P.E.
Isaac Willems
The University of Kansas

Matthew Pierson, Ph.D.
Missouri State University

A Report on Research Sponsored by

THE KANSAS DEPARTMENT OF TRANSPORTATION
TOPEKA, KANSAS

and

THE UNIVERSITY OF KANSAS
LAWRENCE, KANSAS

November 2011

PREFACE

The Kansas Department of Transportation's (KDOT) Kansas Transportation Research and New-Developments (K-TRAN) Research Program funded this research project. It is an ongoing, cooperative and comprehensive research program addressing transportation needs of the state of Kansas utilizing academic and research resources from KDOT, Kansas State University and the University of Kansas. Transportation professionals in KDOT and the universities jointly develop the projects included in the research program.

NOTICE

The authors and the state of Kansas do not endorse products or manufacturers. Trade and manufacturers names appear herein solely because they are considered essential to the object of this report.

This information is available in alternative accessible formats. To obtain an alternative format, contact the Office of Transportation Information, Kansas Department of Transportation, 700 SW Harrison, Topeka, Kansas 66603-3754 or phone (785) 296-3585 (Voice) (TDD).

DISCLAIMER

The contents of this report reflect the views of the authors who are responsible for the facts and accuracy of the data presented herein. The contents do not necessarily reflect the views or the policies of the state of Kansas. This report does not constitute a standard, specification or regulation.

Abstract

Soil nail walls are a widely used technology for retaining vertical and nearly vertical cuts in soil. A significant portion of the cost of soil nail wall construction is related to the construction of a reinforced concrete face. The potential for use of a flexible facing design for soil nail walls to replace reinforced concrete facing was evaluated using three-dimensional finite difference modeling and physical testing of a 1.5 meter by 1.5 meter unit cell of a soil nail wall in clay. A steel mesh form of flexible facing was used as a substitute for concrete. The finite difference model predicted large vertical and horizontal deformations for surcharges of approximately 5 psi. In the physical testing, the flexible facing products performed well with regard to strength, but the facing experienced large vertical and horizontal deformations that were consistent with the numerical modeling. Based on these results, it is recommended that use of flexible facing as a substitute for reinforced concrete be limited to non-critical structures where large vertical and horizontal deformations are acceptable.

Acknowledgements

The authors wish to thank the Kansas Department of Transportation (KDOT) and the KDOT Bureau of Materials and Research for the financial and logistical support they provided for the research described in this report. The authors would also like to thank the University of Kansas Department of Civil, Environmental, and Architectural Engineering (KU CEAE); the University of Kansas Transportation Research Institute and Mr. Jim Weaver of KU CEAE for their participation; and the Geobrugg Company for their supply of materials. Their support is greatly appreciated.

Contents

Tables

Figures

Chapter 1: Introduction

Soil nails are structural reinforcing elements installed to stabilize steep slopes and vertical faces created during excavations. Commonly used soil nails are made of steel bars covered with cement grout. The grout is applied to protect the steel bars from corrosion and to transfer the load efficiently to nearest stable ground. Some form of support, usually wire mesh-reinforced shotcrete, is provided at the construction face to support the face between the nails and to serve as a bearing surface for the nail plates. The use of wire mesh-reinforced shotcrete facing can require the mobilization of a specialty contractor and increase the cost of a project. Use of flexible facing material such as geosynthetic, steel wire, or chain link without shotcrete could provide significant savings. In recent years, alternative forms of facing support for soil nail supported slopes have been used, including steel wire mesh which has been successfully applied in Europe and also gained acceptance in North America. The use of high strength steel wire mesh wire is economical, eliminates the need of drainage, and facilitates the greening of the slopes (Geobrugg 2007).

The mechanism of increased stability of the soil nailed walls can be explained by 1) the increase in the normal force and the shear resistance along the potential slip surface in frictional soil and 2) the reduction in the driving force along the potential slip surface in both frictional and cohesive soils. When the wire mesh is used as a facing material, the mesh and nails act together as a system to provide stability to the slope, preventing deformations in the top layers and restricting movement along planes of weakness. With the high strength of the mesh, it is possible to pre-tension the system against the slope, and the pre-tensioning enables the mesh to provide active pressure against the slope, preventing break-outs between the nails (Geobrugg 2007).

Soil nailing has proven to be an effective and economical means of protecting unstable slopes and providing temporary shoring. Construction facing alternatives such as steel wire mesh and geosynthetic are considered in the present research. A series of FLAC finite difference models were constructed to simulate the performance of nearly vertical soil nail walls with steel wire mesh. The results of the numerical modeling were used to design a large-scale physical

model test conducted in the geotechnical testing box at the University of Kansas laboratory. The large-scale test was conducted on a unit of a soil nail wall with a wire mesh facing.

This report contains a summary of the background of soil nail walls, a description of the modeling and testing, a discussion of the results, and recommendations for use of flexible facing technologies with soil nail walls.

Chapter 2: Literature Review

The major use of soil nailing in the United States to date has been for temporary excavation support for building excavations in urban areas (Byrne et al. 1998). In North America, the first recorded application of the system was in Vancouver, British Columbia in the early 1970s for temporary excavation support (Byrne et al. 1998). The first recorded application of soil nails in Europe (1972–73) is credited to the French contractor Bouygues in a joint venture with the specialist contractor Soletanche for an 18 meter high 70° cut slope in Fontainebleau Sand. The first published use in the United States was the excavation for the foundation of the extension to the Good Samaritan Hospital in Portland, Oregon, constructed in 1976 by a joint venture of Kulchin and Associates, Inc., and Albert K. Leung and Associates (Byrne et al. 1998). Over the last 40 years, many large scale tests have been conducted on soil nail walls, notably the Bodenvernagelung project in Germany that tested a variety of experimental wall configurations (Byrne et al. 1998), the Clouterre project in France, where three large-scale experiments were conducted in Fontainebleau sand by monitoring six full-scale, in-service structures (Plumelle et al. 1990). Since its first use, soil nailing has become a popular form of earth retention, particularly in France and Germany, and has become common practice in some U.S. cities. The application of soil nailed walls in South Asia is also increasing rapidly because of its inherent advantages of speed and simplicity in construction (Wong et al. 1997).

Plumelle et al. (1990) carried out a full-scale test of soil nails on Fontainebleau sand. The soil nailed walls were failed by saturation of soil, decreasing the adherence length of the bars, and progressively increasing the height of excavation. The lateral earth pressure was above the coefficient of earth pressure at rest (Ko) at the beginning of the construction of the soil nails at the top and below the active state of stress (Ka) at the lower sections. Due to creep, at the end of three months, there was tensile force generated at the lower nails. At failure, a fissure on the top surface was observed at 35% of the height of the excavation back from the face. Vertical and lateral deformations were nearly equivalent at approximately 0.3% of the wall height. It was also reported that the bending stiffness of the soil nails were mobilized under large deformations.

Wong et al. (1997) conducted research on the field performance of soil nailed walls constructed in the residual soils of Singapore. Drill holes 100 mm in diameter were made using an augur bit at 15° inclination to the horizontal, the grid size was 1 m by 1 m (V × H) and the length of nail was 7 m. The 200 mm thick facing was constructed with 100 mm reinforced and 100 mm unreinforced shotcrete. Weep holes were provided for drainage. The study found that forces in all nails increased during the post construction period. In the nine-month period there was only a slight increase in nail forces in the top four rows; however, the lower three rows experienced a significant increase in the nail force. After three years, the maximum displacement at the crest of the wall was 37 mm, and the toe of the wall was 4 mm. The maximum lateral displacement was within 0.4% of the total wall height. The performance over the test period showed that the nailed wall demonstrated satisfactory performance under dynamic loading cycles.

Yuan et al. (2003) developed a new approach to limit equilibrium method that computes the interslice forces by recursion and fulfills the equilibrium requirement for interslice forces of the last boundary slice by iteration. This study conducted a parametric study on the effect of soil behavior and the arrangement pattern of nails on the factor of safety and reliability index. Parametric study showed that the shear strength of the soil had a larger effect on the factor of safety and the reliability index of soil nailed walls.

Alston and Crowe (1993) presented case histories relating to the design and construction of two retaining wall systems constructed at a site consisting of dense to very dense sandy silt with the ground water table at great depth and another site consisting of hard silty clay till of low plasticity. Both potentially unstable slopes were supported satisfactorily, economically, and safely by the installation of near-horizontal ground reinforcement systems in areas that are not accessible by conventional soil nail installation equipment. This study also showed that the use of soil nails can eliminate the problems associated with the conventional earth retaining structures near property lines. In these sites geogrid was used to connect the soil nails and the facing wall made of dry stone.

Geobrugg (2007) found that the low tensile strength of conventional wire mesh has led to the use of steel wire rope nets, but these nets tend to be relatively expensive. This paper showed

that these limitations are overcome by the development of a cost-effective diagonal wire mesh manufactured from high tensile strength, highly corrosion-resistant wire. In extensive testing, this mesh demonstrated a strength approaching that of wire rope nets. This study also recommended the use of anchor plate that optimizes force transfer from mesh to anchors that allow the mesh to be pre-tensioned against the slope, which restricts deformations in critical surface sections and prevents movement along planes of weakness. Anchored slope stabilization systems using high strength steel wire mesh as a facing material was found to be an effective and economical means of protecting unstable slopes and providing temporary shoring.

The Federal Highway Administration (FHWA) has published a comprehensive manual for design and construction monitoring of soil nail walls (Byrne et al. 1998). However, efforts are continuing to make this technology more effective and economical.

2.1 Construction Sequence

The construction of a soil nail wall is an iterative top-to-bottom process. A typical sail nail wall construction sequence is shown in Figure 2.1 (Byrne et al. 1998). Though there are multiple alternatives for the final step (step 6), CIP (cast in place) concrete is most often used for the final facing.

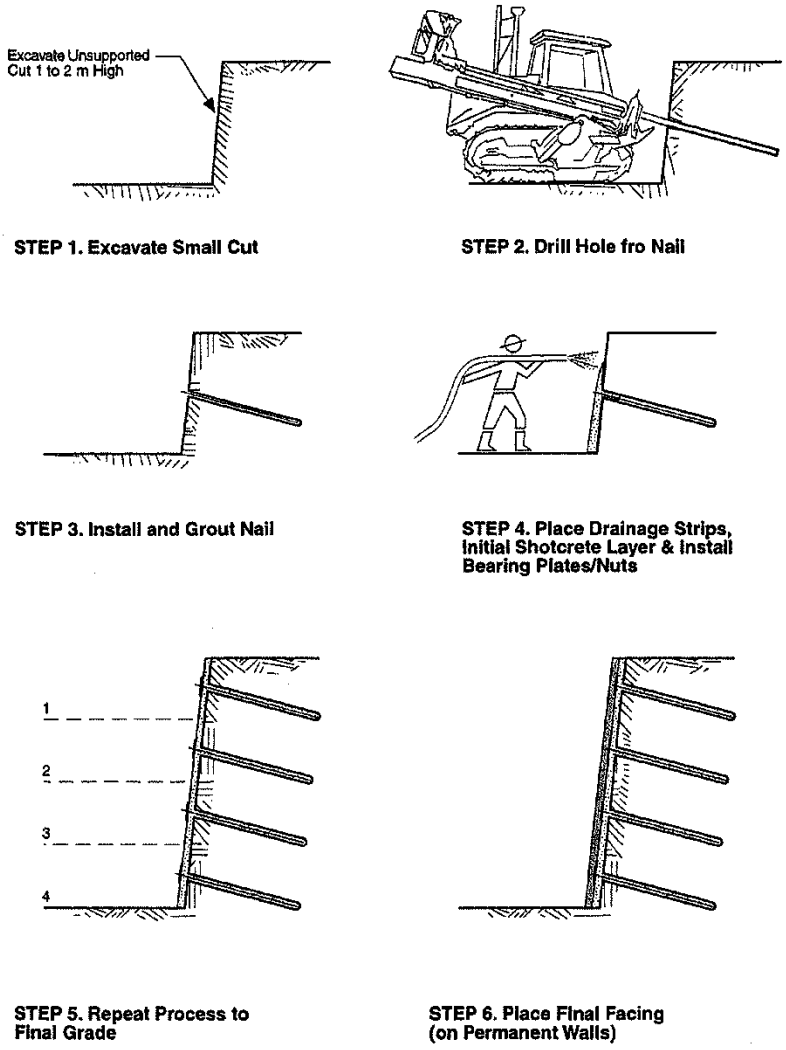

FIGURE 2.1
Typical nail wall construction sequence (Byrne et al. 1998)

2.2 Behavior of Soil Nails

The soil behind the wall face is divided into active and resistant zones. The portion of the slope that would fail without reinforcement is the active zone as shown in Figure 2.2. Soil behind the active zone is in the resistive zone. These areas are separated by the slip surface. A soil nail wall acts to tie the active zone (that would otherwise fail by moving outwards and downwards with respect to the resistant zone) to the resistant zone.

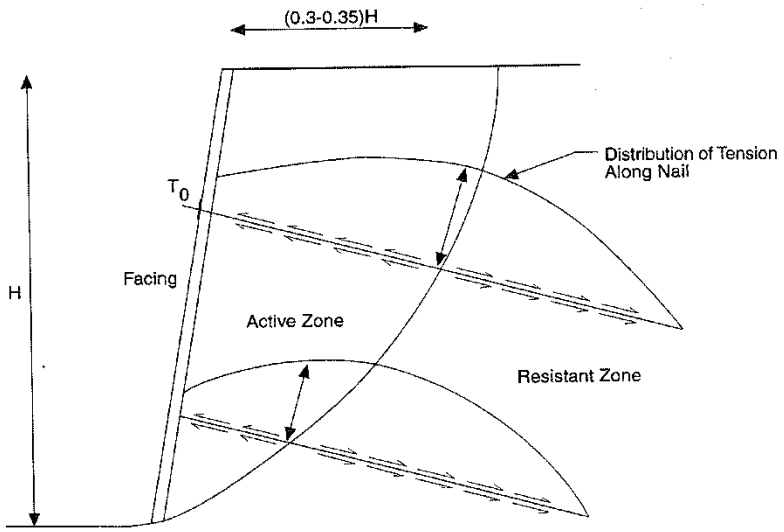

FIGURE 2.2
Conceptual soil nail behavior (reproduced from Byrne et al. 1998)

2.3 Soil Nail Wall Failure Modes

There are three generic failures that can occur in a soil nail wall: nail tendon failure, pullout failure, and face failure (Byrne et al. 1998).

- **Face failure.** Face failure occurs when the face or the connection to the face fails from shear or flexure as shown in Figure 2.3a. Specific failure mechanisms include flexure, punching shear, and failure of headed studs in tension for a permanent wall facing headed-stud connection system.
- **Pullout failure**. Pullout failure occurs when the soil nails do not extend far enough into the resistant zone to mobilize sufficient resistance to retain the face as shown in Figure 2.3b and the soil nails pull out of the resistant zone.

- **Nail tendon**. Nail tendon failure occurs when the tensile strength of the nail is exceeded by the maximum tensile stress (T_N) (Figure 2.3c). Once this occurs, the nail breaks in tension causing failure.

For both nail tendon failure and pullout failure, most conventional design methods utilize a method of slices and assume interslice forces to be zero. Other methods may include these forces, such as the JC method presented in the *New Approach to Limit Equilibrium and Reliability Analysis of Soil Nail Walls* (Yuan et al. 2003).

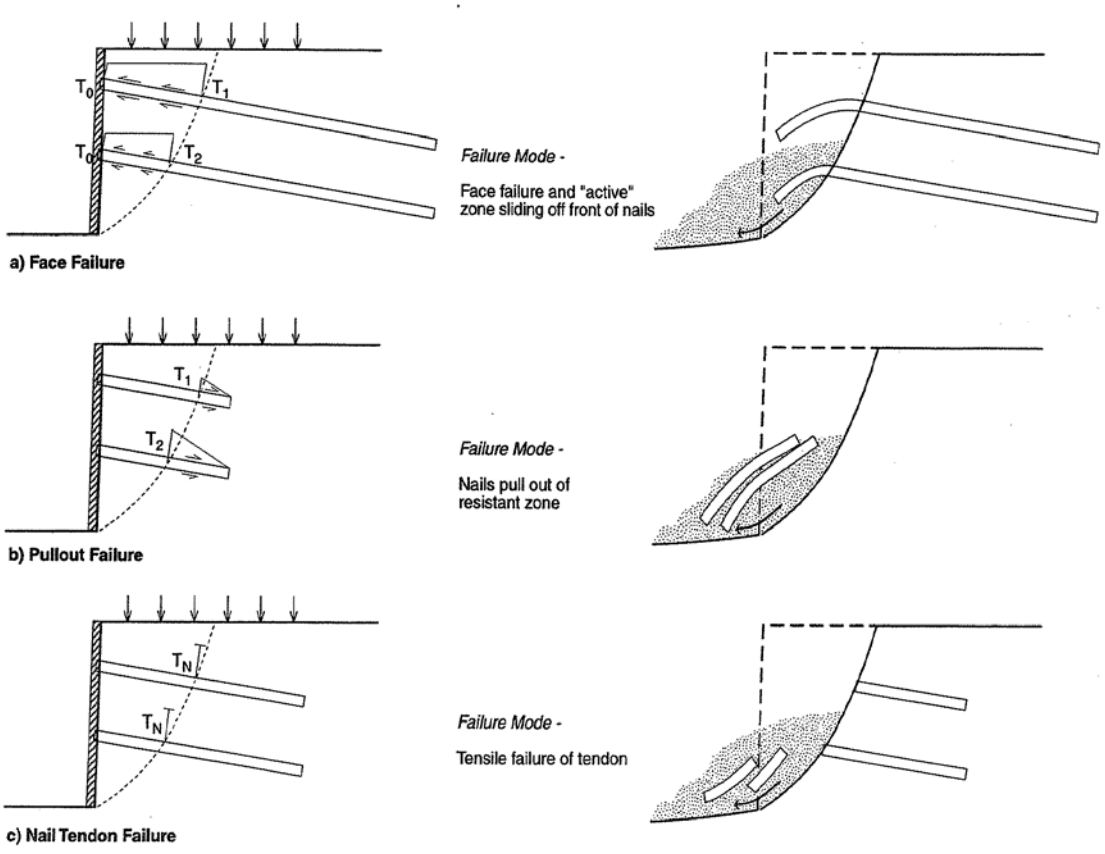

FIGURE 2.3
Potential soil nail wall failure modes (reproduced from Byrne et al. 1998)

2.3.1 Further Investigation of Face Failure

The stress along the face of the of the soil nail wall is not uniformly distributed. The stress is greater closer to the nail head location as seen in Figures 2.4 and 2.5 (Byrne et al. 1998).

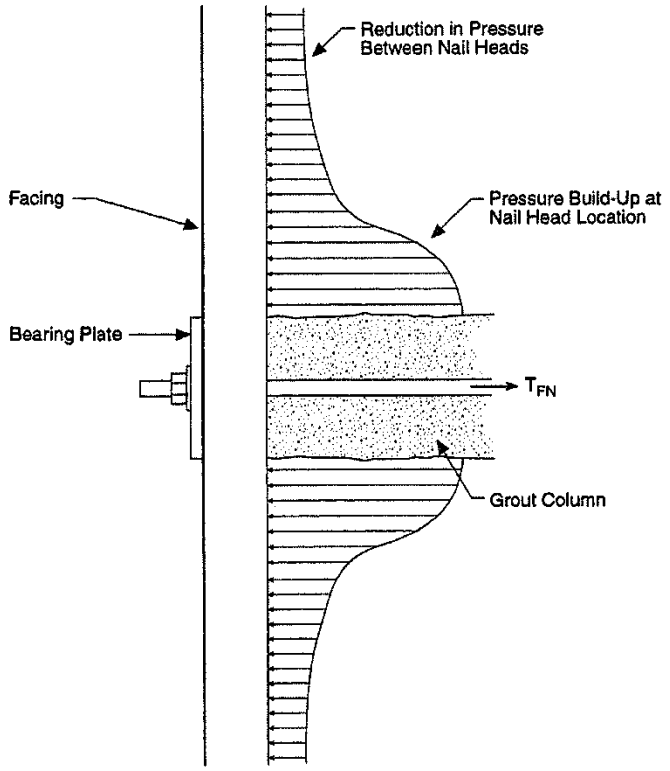

FIGURE 2.4
Typical facing pressure distribution (reproduced from Byrne et al. 1998)

2.3.2 Flexural Strength of the Facing and Punching Shear Strength

Since the pressure is not uniform across the facing, the equation of the nominal resistance of the facing must take into consideration both the peak pressure and the lowest pressure. Equations have been developed to calculate the flexural, punching shear, and nail head strength for rigid facing and are available (Byrne et al.1998).

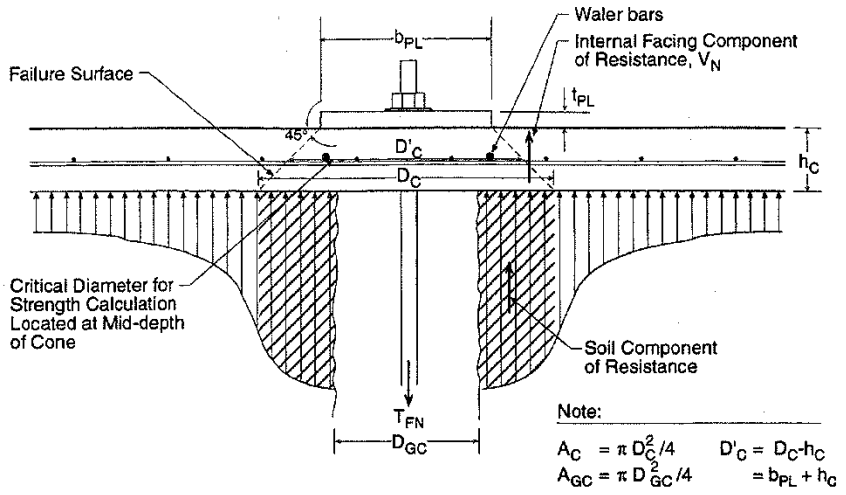

Temporary Bearing-Plate Connection

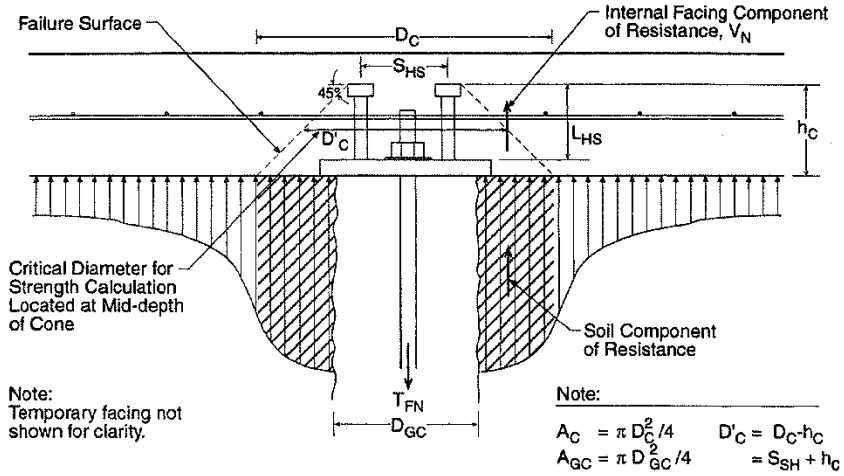

Permanent Headed-Stud Connection

FIGURE 2.5
Punching shear of nail head connections (reproduced from Byrne et al. 1998)

Chapter 3: Finite Difference Modeling

Numerical modeling of the soil nailed wall was conducted using FLAC3D. The numerical modeling was run for multiple surcharge levels below 15 psi. The results of the 4 and 5 psi surcharge loading were close to the failure surcharge obtained by the physical test, so these two cases are discussed here.

Models were developed for 4 and 5 psi surcharges for both short- (undrained) and long-term (drained) scenarios. The properties of soil, plates, geogrid, cable, and grout used for the numerical modeling under both the short- and long-term scenario are given in Table 3.1. Contours of displacement of the wall under a 4 psi surcharge are shown in Figure 3.1 for the short-term loading condition and Figure 3.2 for the long-term loading condition. Under both loading conditions, the displacements for the lower row of soil nails were not significant. However, for the long-term loading condition, both vertical and horizontal displacements were significant near the top row of soil nails. Figures 3.3 and 3.4 show the displacement contours at 5 psi surcharge under short-term and long-term loading conditions, respectively. For a 5 psi surcharge, the results showed similar displacement trends as observed in case of the physical model test explained in Chapter 5 of this report; soil near both the upper and lower rows of soil nails experienced significant deformation for both horizontal and vertical directions. Long-term grid stress under a surcharge of 5 psi obtained from the model test is shown in Figure 3.5. Higher stresses are seen on the upper portion of the wall, which is consistent with magnitude of deformation observed from both the physical test and FLAC modeling.

TABLE 3.1
Summary of parameters used for the numerical modeling

Fill	**Long-term**		**Short-term**
Unit Weight	125	pcf	
Friction Angle	34	deg.	
Cohesion	104	psf	942
Model	Mohr-Coulomb		
Young's Modulus	37.4	ksi	
Poisson's Ratio	0.285		
Plates			
Unit Weight	125	pcf	
Model	Elastic		
Young's Modulus	37.4	ksi	
Poisson's Ratio	0.285		
Interface Friction Angle	10	deg. Applied to the test box sides	
Geogrid			
Stiffness	144000	lb/ft	
Interface Friction Angle	51	deg.	
Cable			
Stiffness	4500000	Kip	
Area	1.076	ft^2	
Modulus	29000	ksi	
Yield Force	225000000	kip	
Grout			
Unit Weight	125	pcf	
Cohesion	2	psf	
Friction angle	35		
stiffness/unit length	480	kip/ft	
Radius	0.522	ft	

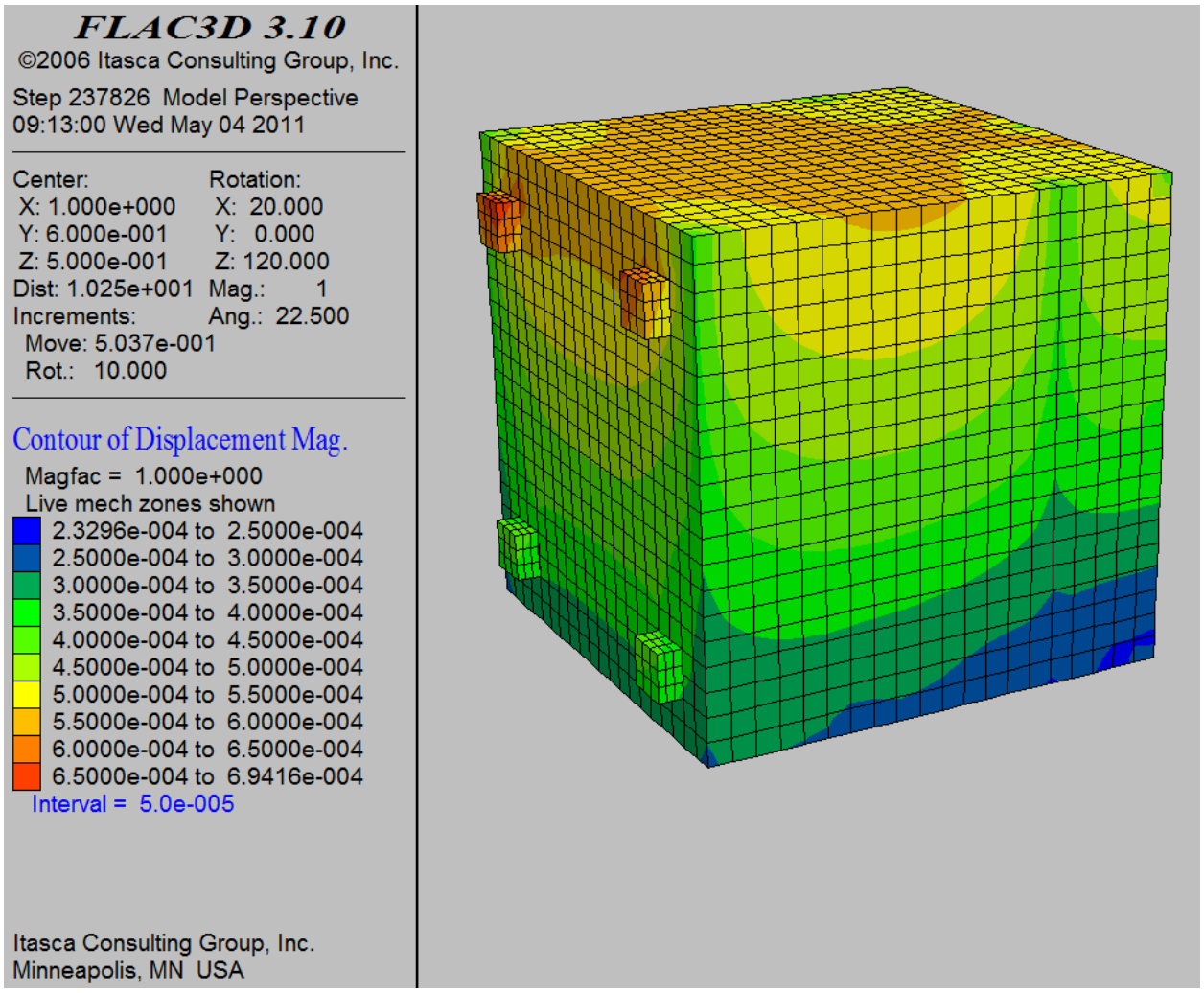

FIGURE 3.1
Contour of the displacement of the soil nailed wall at 4 psi surcharge application for the short-term condition (displacements in m)

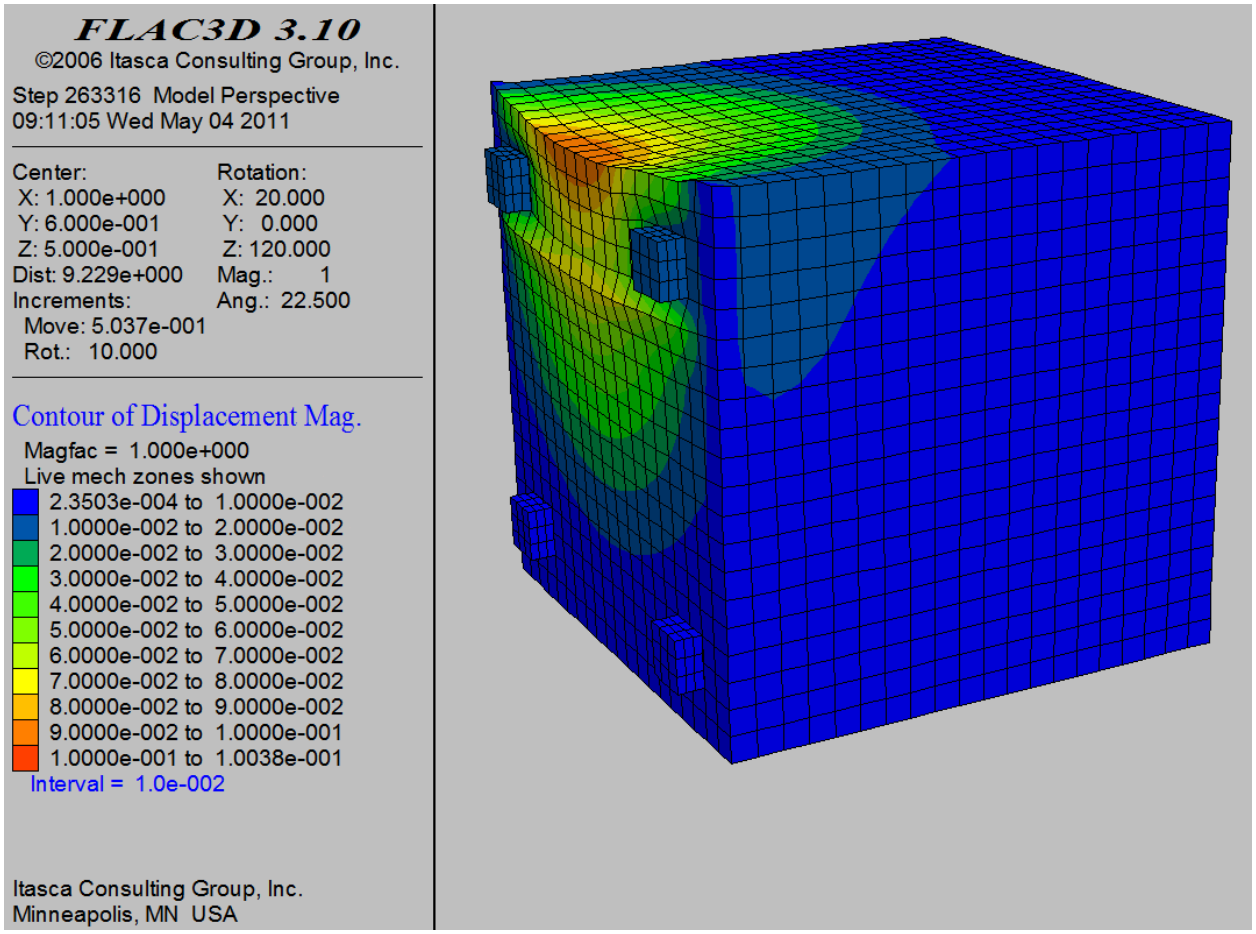

FIGURE 3.2
Contour of the displacement of the soil nailed wall at 4 psi surcharge application for the long-term condition (displacements in m)

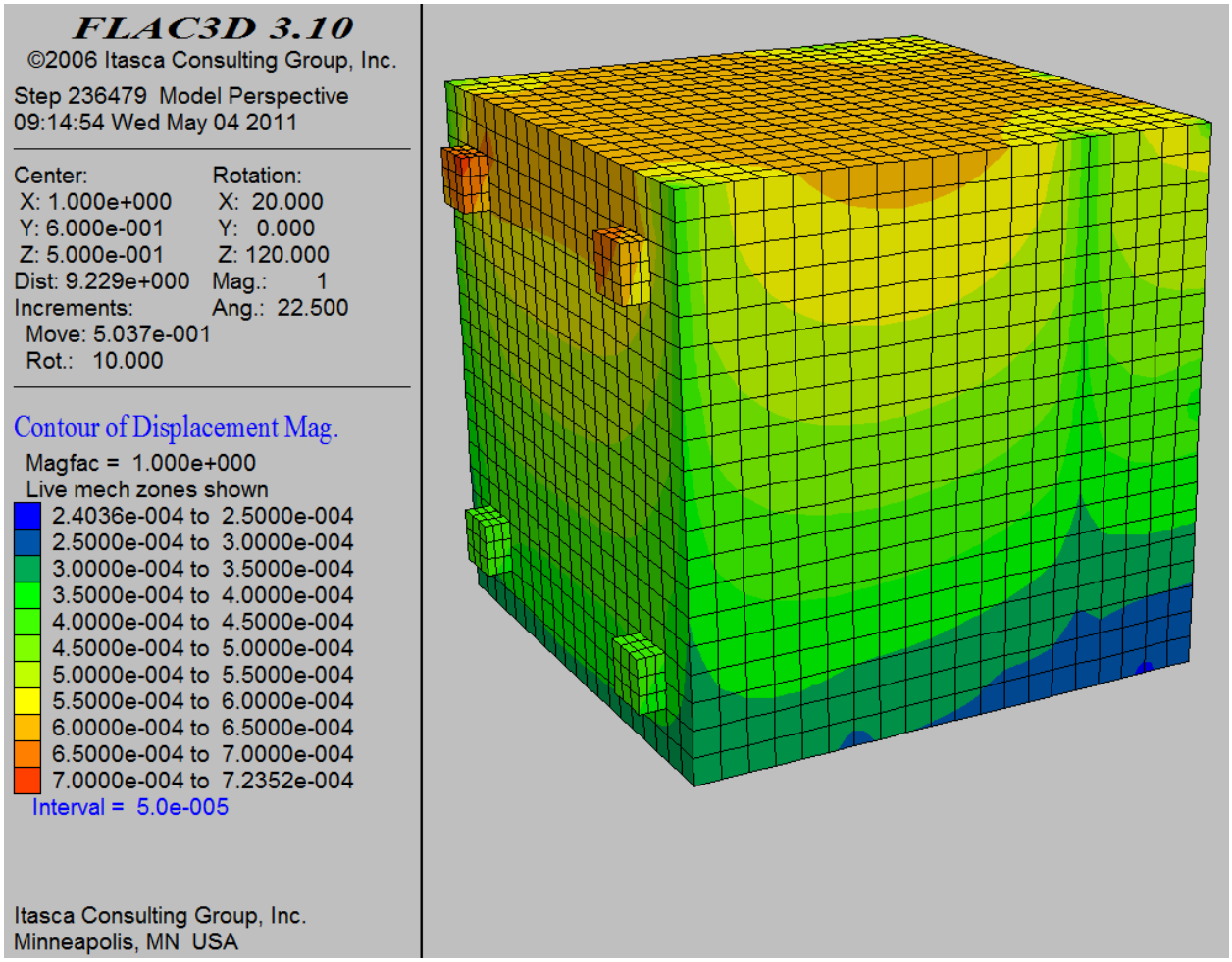

FIGURE 3.3
Contour of the displacement of the soil nailed wall at 5 psi surcharge application for the short-term condition (displacements in m)

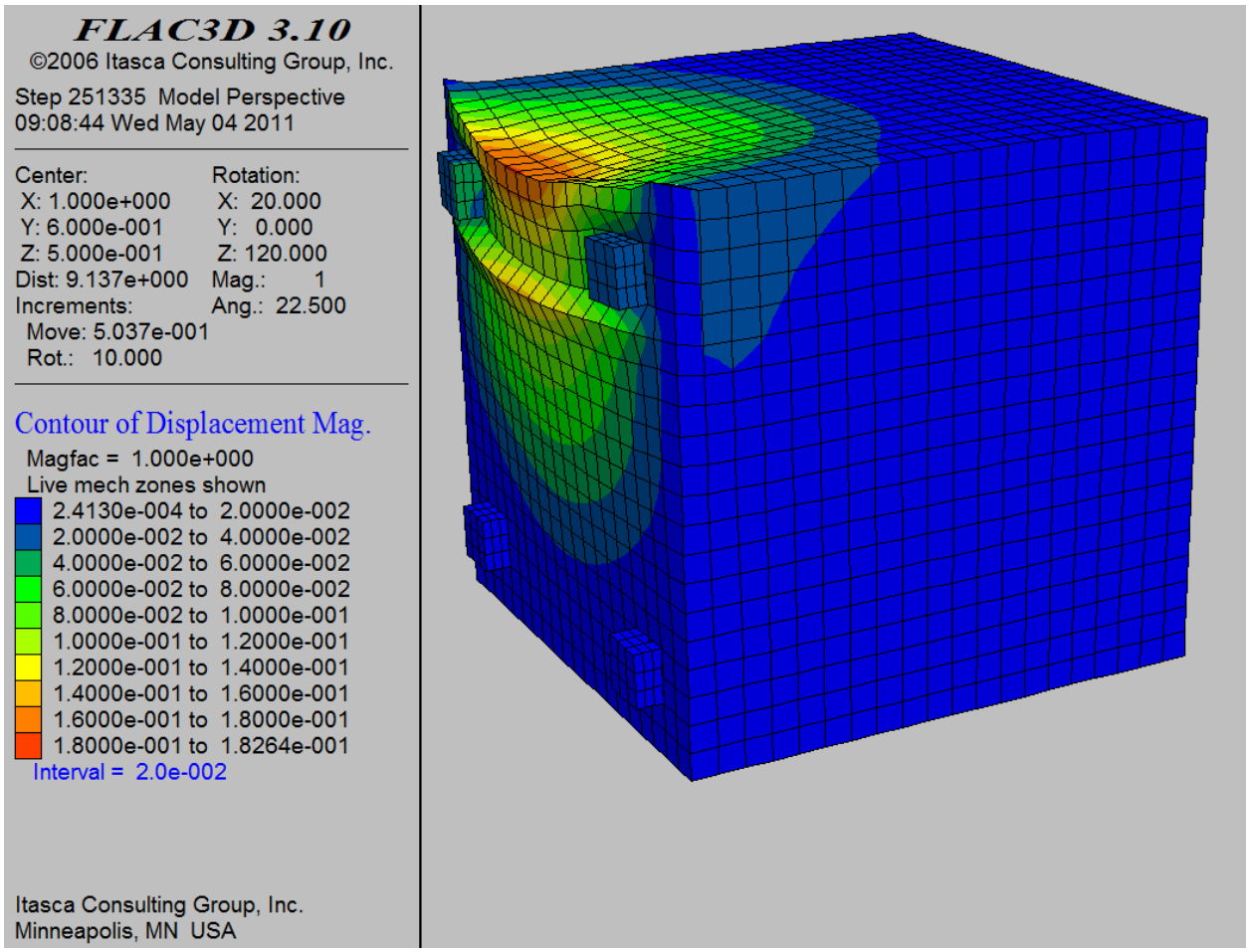

FIGURE 3.4
Contour of the displacement of the soil nailed wall at 5 psi surcharge application for the long-term condition (displacements in m)

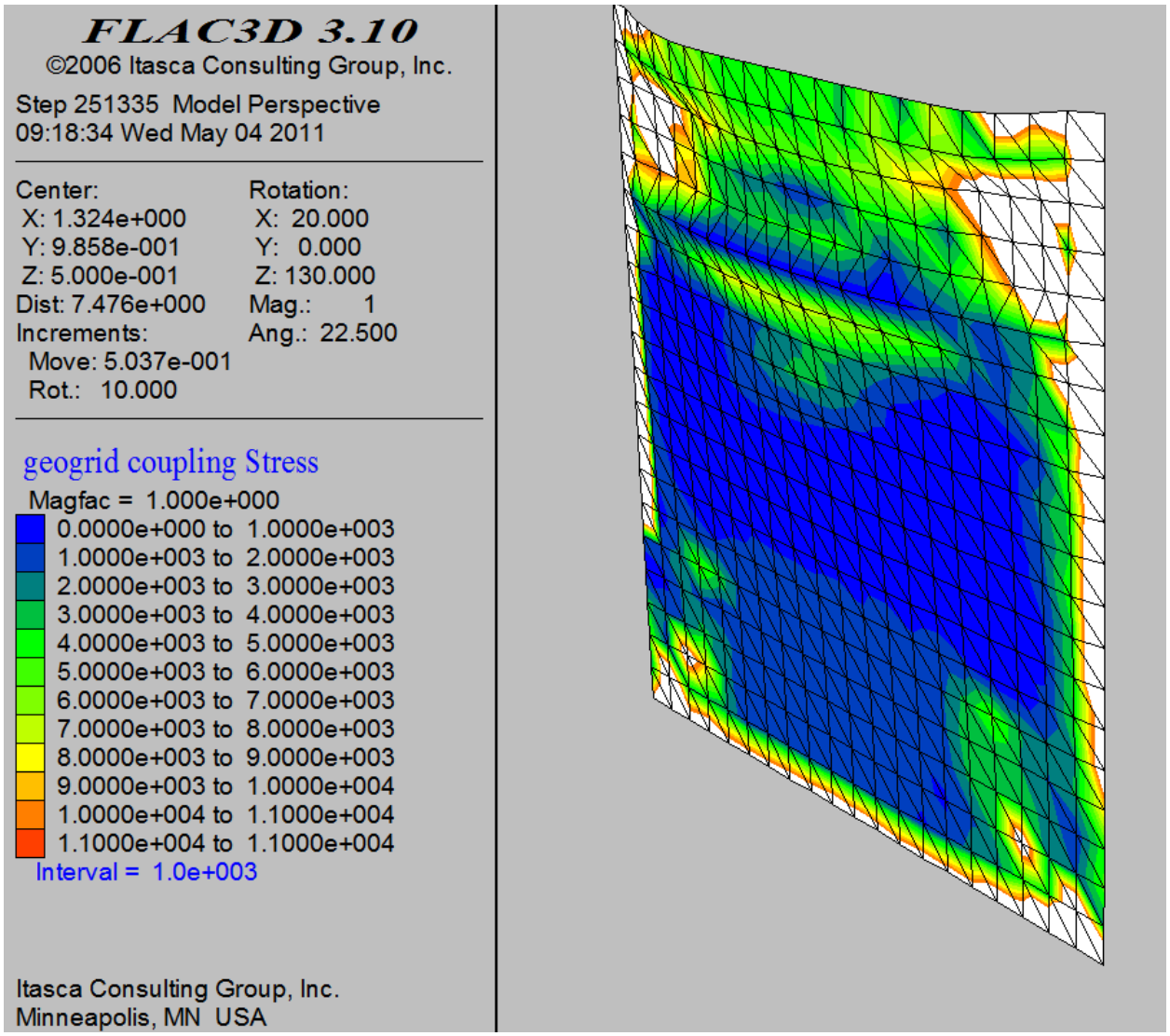

FIGURE 3.5
Long-term grid stress on the soil nails wall facing for a 5 psi surcharge application for the long-term condition (units in kPa)

The forces acting along the length of the soil nails obtained from the FLAC numerical modeling under short-term and long-term conditions for 4 psi are shown in Figures 3.6 and 3.7 and for 5 psi in Figures 3.8 and 3.9. In all the cases, the soil nails at the upper row were subjected to higher tensile force compared with the lower layer of nails. It was more evident in case of long-term loading. These relative results are consistent with strain measurements observed from the physical model test which will be discussed in Chapter 5 of this report and shown in Figure 5.25.

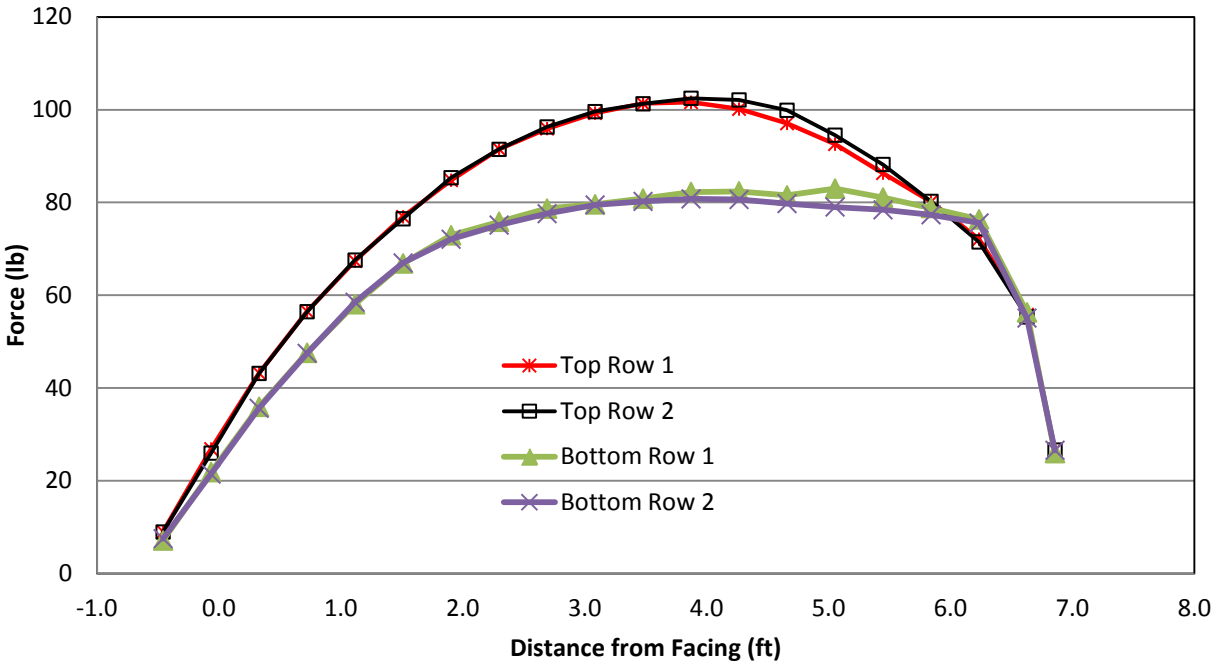

FIGURE 3.6
Force acting along the length of the soil nails at 4 psi surcharge application for the short-term condition

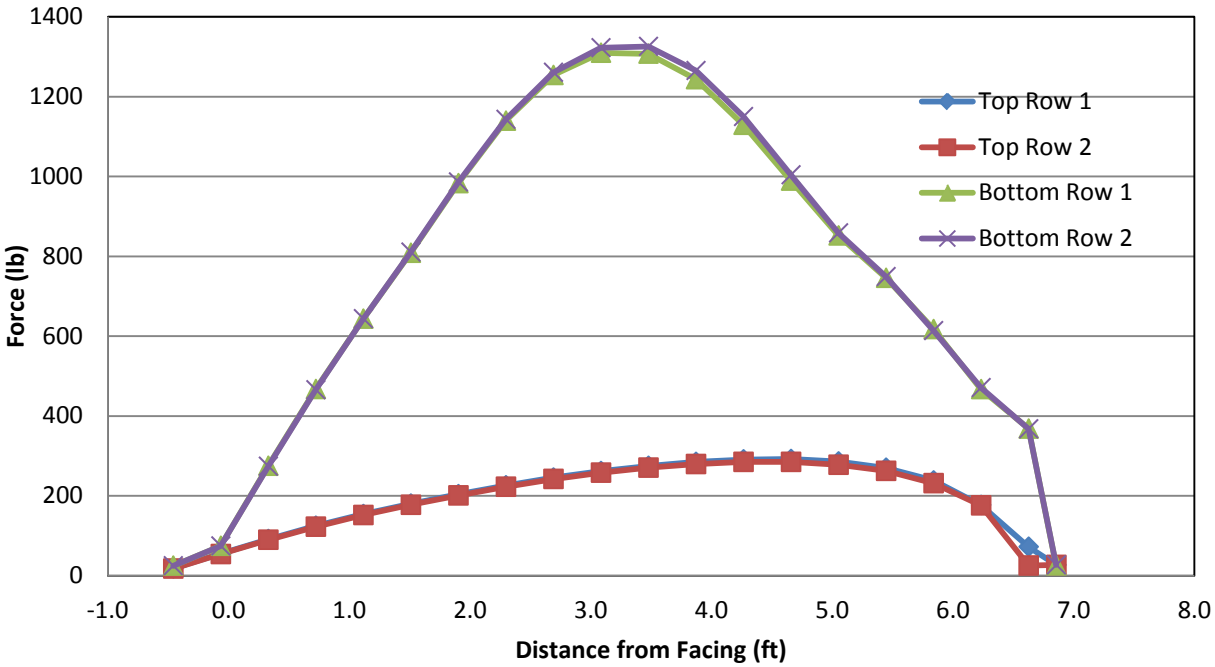

FIGURE 3.7
Force acting along the length of the soil nails at 4 psi surcharge application for the long-term condition

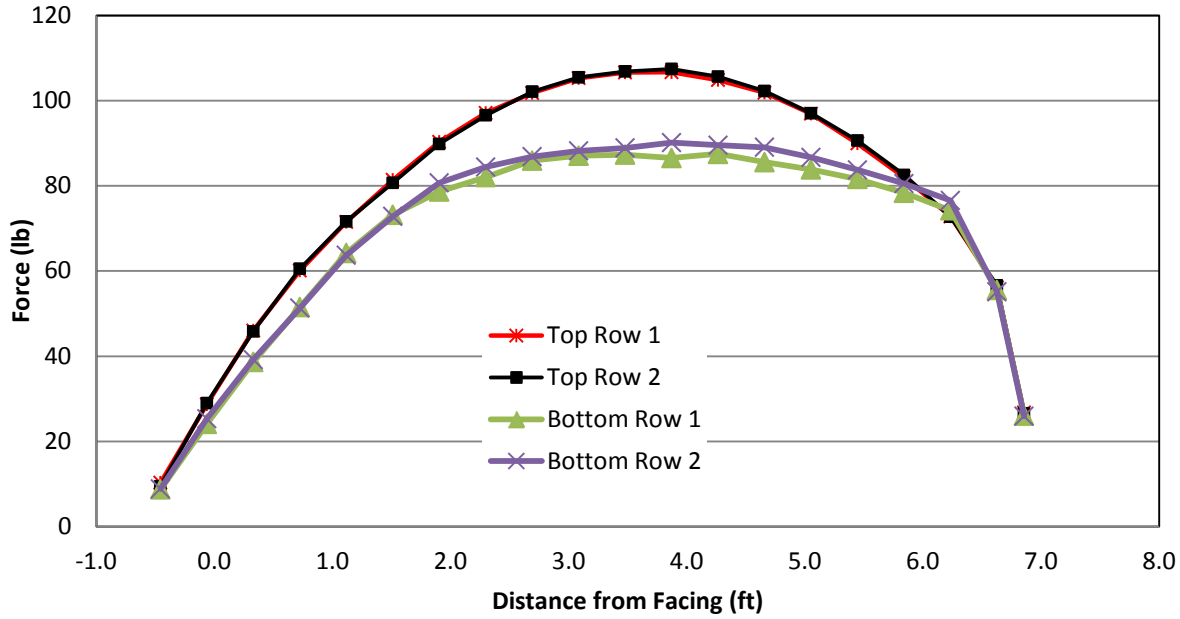

FIGURE 3.8
Force acting along the length of the soil nails at 5 psi surcharge application for the short-term condition

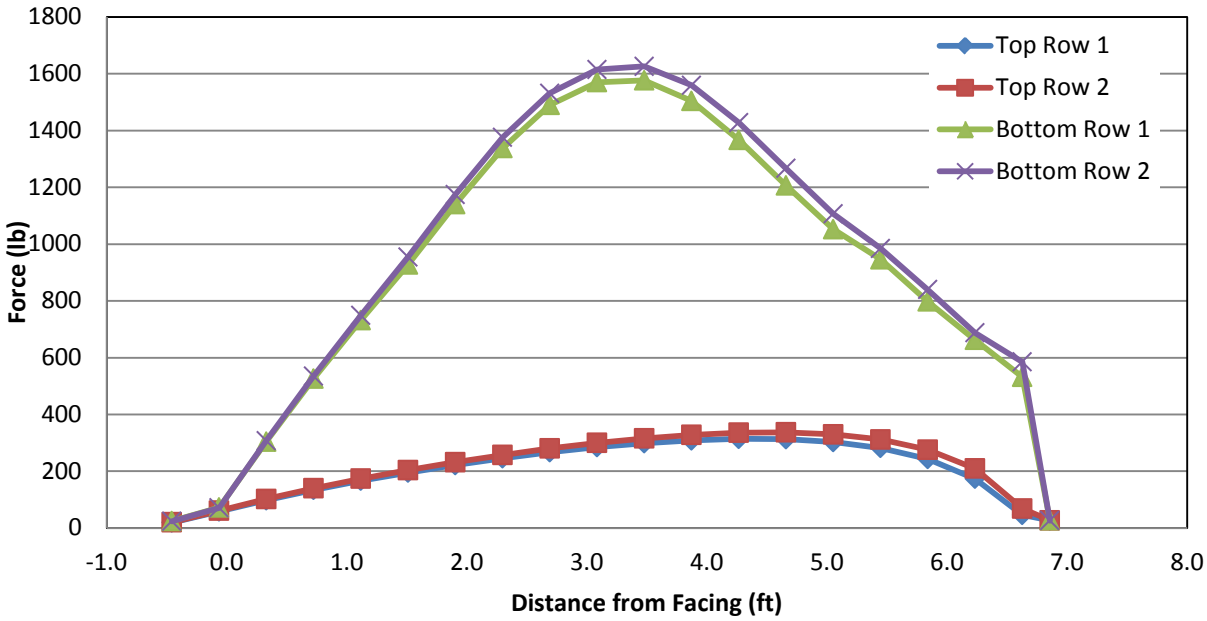

FIGURE 3.9
Force acting along the length of the soil nails at 5 psi surcharge application for the long-term condition

Chapter 4: Physical Testing Materials and Equipment

This chapter contains a discussion of the materials and test equipment used for the physical testing. The physical test was designed to model a unit of a typical soil nail wall with a nail spacing of 5 ft by 5 ft (1.5 m × 1.5 m). A surcharge was applied to simulate the effect of additional wall height above the unit being tested. Significant deformation was expected based on the finite difference modeling; therefore, a wire mesh (chain-link) form of facing was used, because it was expected to produce the lowest deflection of the flexible facing options.

4.1 Materials used during testing

Clay from the Lawrence, Kansas, area that had been used as retained fill was used to construct the soil wall. The soil is shown in Figure 4.1. This clay had a liquid limit of 55 and plastic limit of 25, resulting in a plasticity index of 30. The soil was classified as A-7-6 (AASHTO System) and CH (USCS). The specific gravity of the clay material was 2.71, and the grain size distribution is shown in Figure 4.2. Standard Proctor compaction and unconfined compression tests on this soil were carried out in the laboratory. The optimum moisture content and the maximum dry density were 24% and 98.3 lb/ft^3 (1.576 Mg/m^3), respectively. The Standard Proctor compaction curve and the unconfined compression tests results are shown in Figures 4.3 and 4.4, respectively. Table 4.1 shows the results of three unconfined compression tests. Based on the test results of the Standard Proctor compaction test, the target for the soil compaction was set at a minimum of 90% of standard compaction and a moisture content 2% wet of optimum.

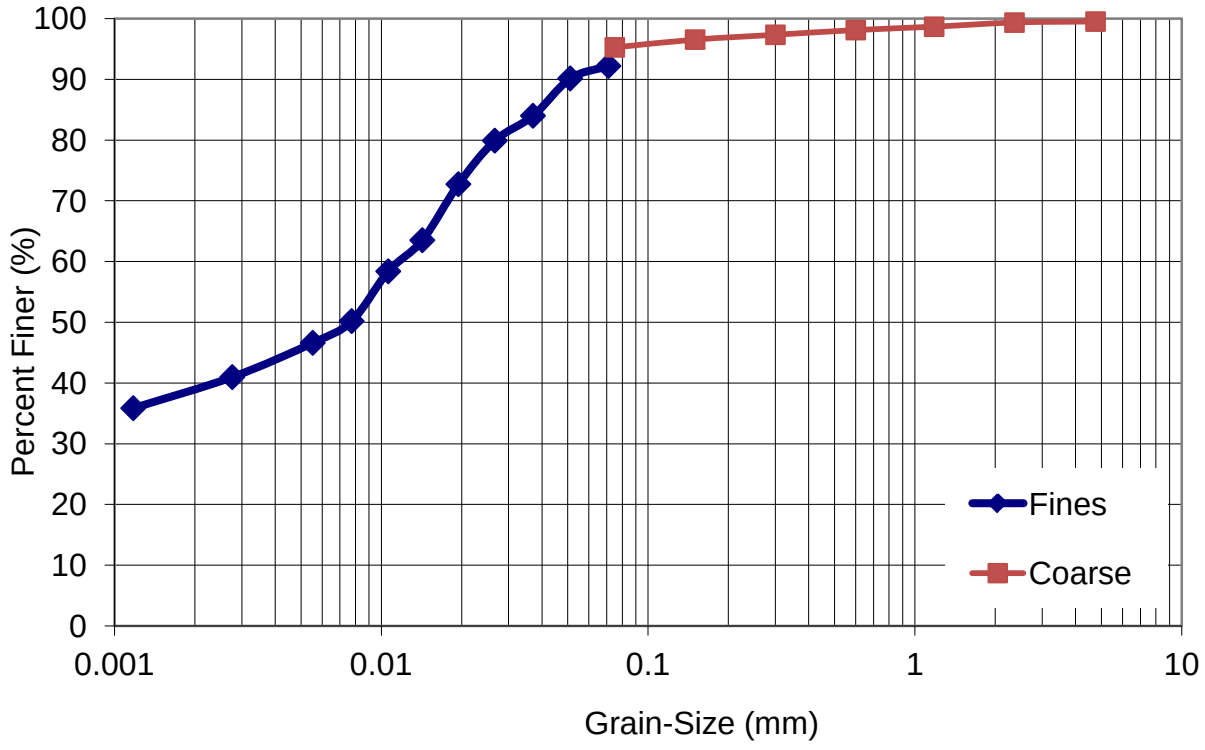

FIGURE 4.1
Grain size distribution of test soil

FIGURE 4.2
Soil used as fill material for the soil nailed wall

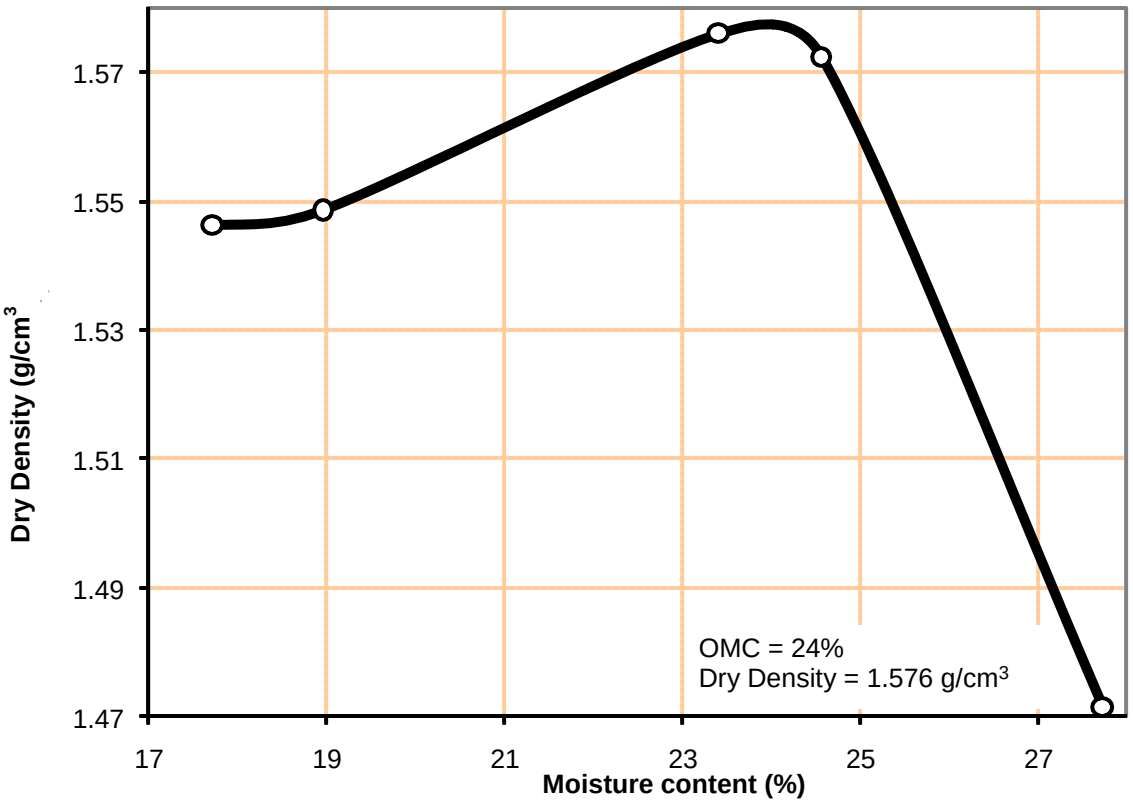

FIGURE 4.3
Compaction curve of soil

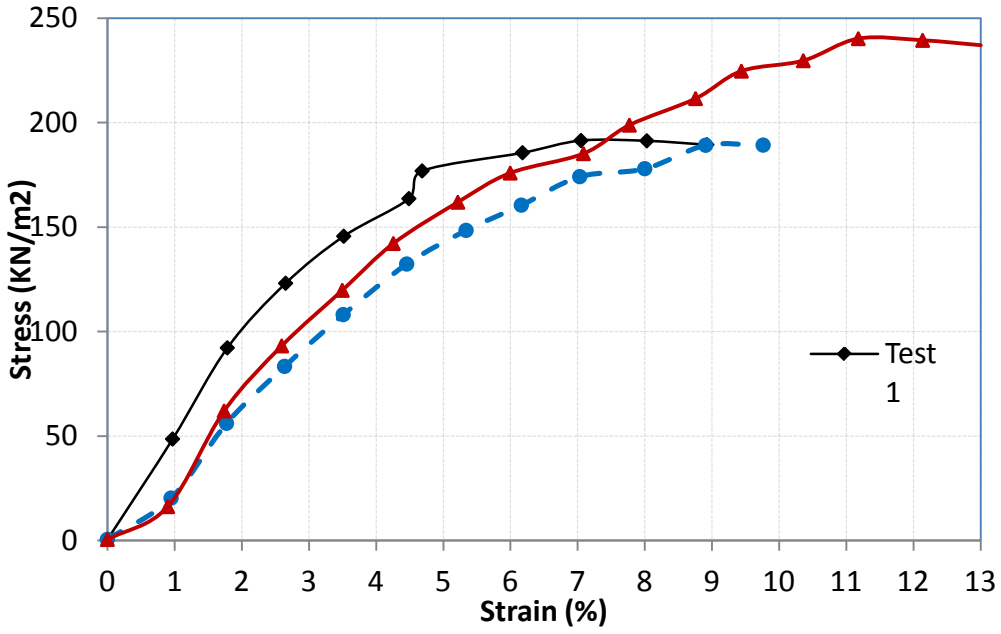

FIGURE 4.4
Unconfined compression test results

TABLE 4.1
Result of the unconfined compression testing

Sample	Length (mm)	Area (mm^2)	Mass (gm)	Moisture (%)	q_u (kN/m^2)	$S_u = q_u/2$ (kN/m^2)	q_u (psf)	$S_u = q_u/2$ (psf)
1	72.1	862.9	121.9	24.8	191	96	3997	1999
2	71.5	864.3	121	25.2	189	95	3951	1976
3	71.8	865.1	122.1	24.7	240	120	5017	2508

Four soil nails were used in the test. The nails, places, and wire mesh were supplied by Geobrugg. The soil nails were 0.959 inch diameter threaded steel bars. The elastic modulus of the steel bars used for soil nails was 29,000,000 psi. For an actual wall, the soil nails are grouted with cement, so for the test wall the steel bars were covered with 6 inch diameter cement concrete prior to construction. The soil nails are shown in Figure 4.5. Two steel plates with connecting chain links were fixed at the back of the test box as shown in Figure in 4.6, which served as the anchor for the soil nails. The picture of the chain link connections are shown in Figure 4.7. Figure 4.8 shows the stress–strain curve of the steel rod used as soil nails.

FIGURE 4.5
Soil nails

FIGURE 4.6
Anchor steel plates

FIGURE 4.7a
Chain link on the anchor plates

FIGURE 4.7b
Chain link on the soil nails

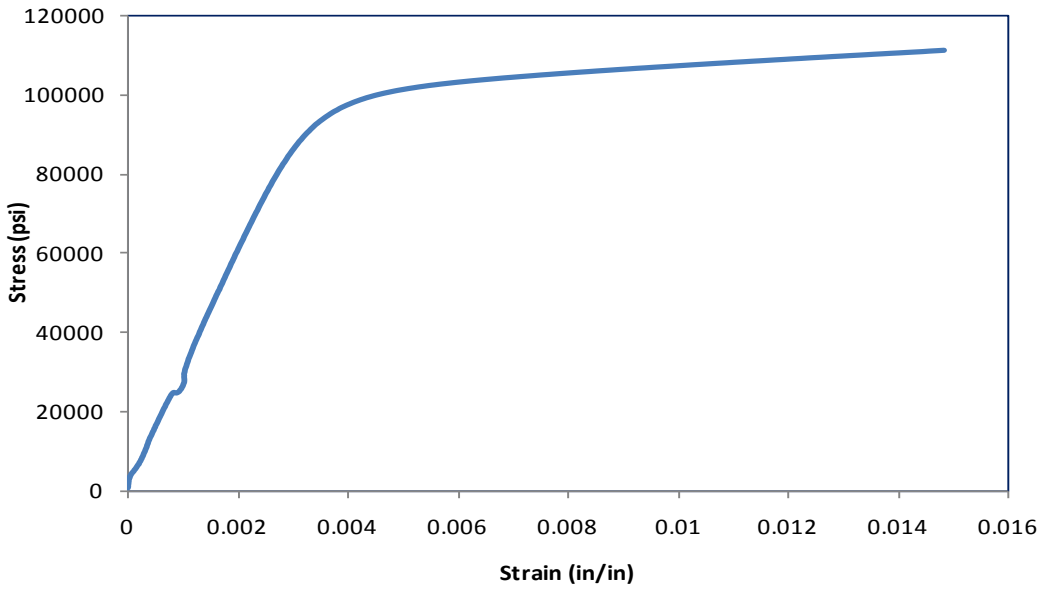

FIGURE 4.8
Strain-Stress curve of the steel bar used in the soil nails

A 3.5 oz (99.65 g) non-woven geotextile was used between soil and the galvanized wire mesh. The picture of the geotextile, wire mesh, and connection to the soil nails are shown in Figures 4.9 and 4.10. The spike plates seen in these figures are made of galvanized iron and have dimensions of 13.0 inch by 7.5 inch by 0.4 inch (330 mm × 190 mm × 10 mm).

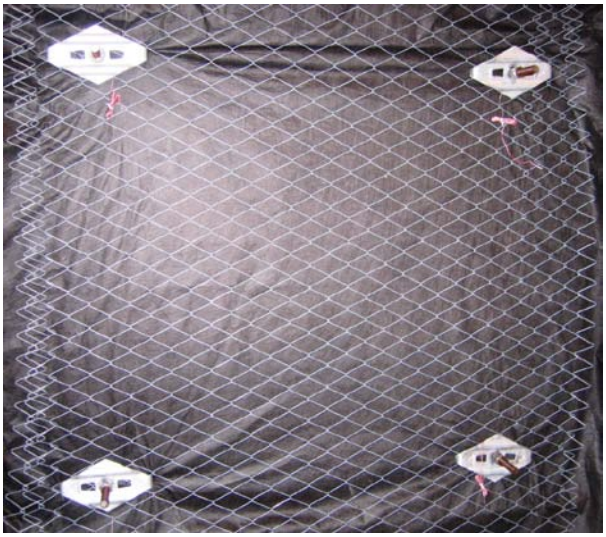

FIGURE 4.9
Galvanized wire mesh and geotextile at the front face of the soil nailed wall

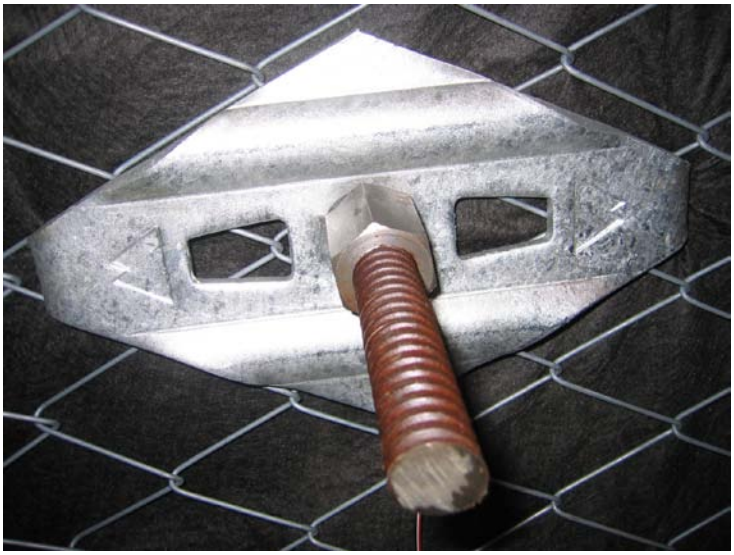

FIGURE 4.10
Spike plate (bearing plate) attached at the end of the soil nails

After completing the construction of the fill, a geosynthetic drainage layer was placed on top of the soil wall as shown in Figure 4.11 with the permeable side down. A set of tubes attached to a water supply was distributed throughout this layer to introduce simulated rainfall in the event the wall was not failed during the initial loading procedure.

FIGURE 4.11
Drainage layer

4.2 Equipment and Test Box

Figure 4.12 show the picture of the large steel geotechnical testing box. Three sides and the base of the box are fixed, while the front side of the box has detachable steel channel sections of height 15 cm fixed with nuts and bolts. The size of the box is 2.2 m by 2 m by 2 m (L × B × H).

A servo hydraulic MTS loading system consisting of a loading frame, a hydraulic actuator, and a servo-control unit connected to both a data acquisition system and a hydraulic control valve was used to apply the load on test sections in the large geotechnical testing box. The load actuator has a 55 kip (245 kN) capacity, which is equivalent to a surcharge of approximately 7 psi. The MTS loading actuator is seen on Figure 4.12 hanging from above the center of the geotechnical box.

FIGURE 4.12
Large geotechnical test box

Half-square grid general purpose strain gages were used in the tests. The strain gages had grid resistance of 120.0 ± 0.6 ohm, grid length of 6.35 mm, and grid width of 3.18 mm. One strain gage each was affixed on each soil nails. The strain gages were all fixed on the top part or the nail. A smart dynamic strain recorder (DC-204R) was used to record the strain data from all the strain gages. The strain gages were fixed on the steel rods as shown in Figure 4.13.

FIGURE 4.13
Strain gage connected to the soil nail

Four string potentiometers (string pots) were used to measure the horizontal movement of the soil face. The string pots are shown in Figure 4.14. Geofoam panels were used to uniformly distribute/transfer the applied load from the steel loading plate to the top of the soil wall. Figures 4.15 and 4.16 show the geofoam and a drawing of the loading plate. Figure 4.17 shows the application of load from the MTS actuator to the steel plate at the top.

FIGURE 4.14
String pots

FIGURE 4.15
Geofoam

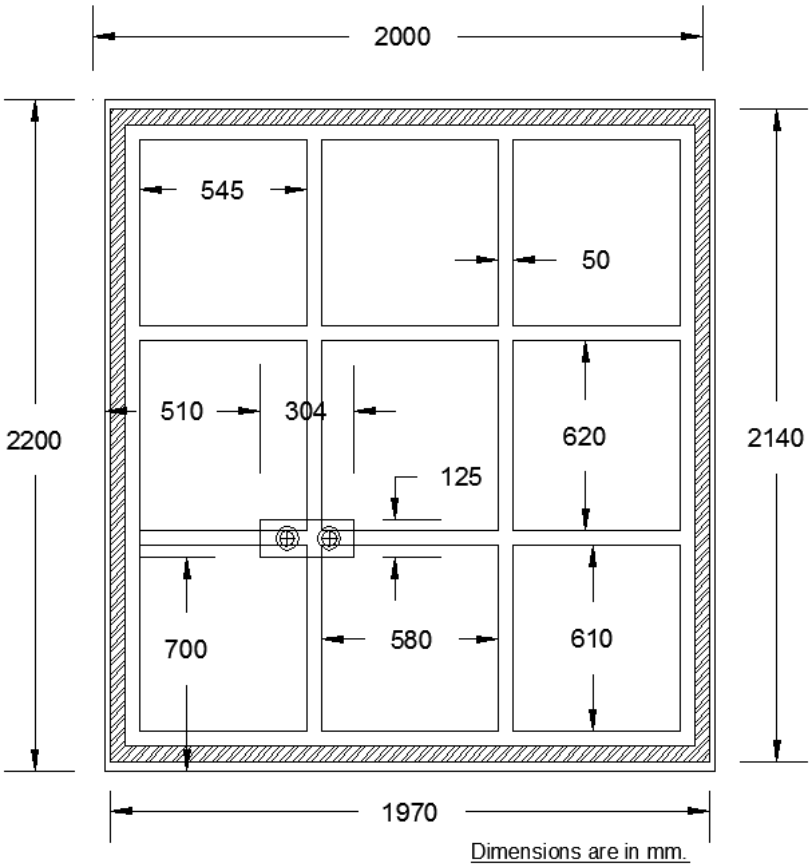

FIGURE 4.16
Steel plate placed on the top of the soil-nailed wall

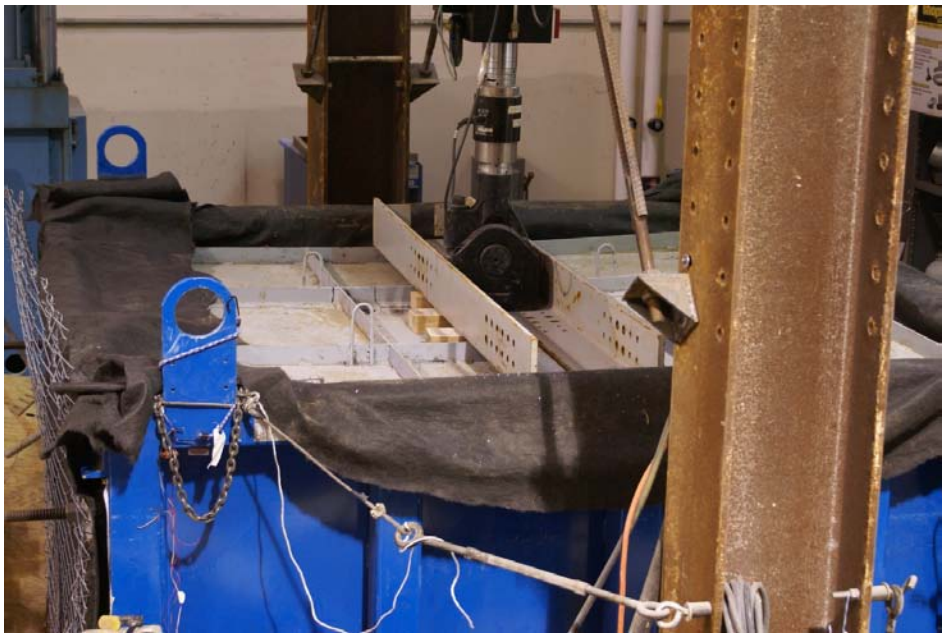

FIGURE 4.17
Surcharge application by the MTS loading actuator

Chapter 5: Physical Testing

5.1 Installation and Test Sequence

1. The geotechnical test box was filled with the test clay in 15 cm (6 inch) lifts. The front side of the box was removed and the geotextile and wire facing was installed.
2. Two steel plates (Figure 4.5) welded with chain links to anchor (Figure 4.6a) the soil nails were installed at the back side of the box. The chain links were welded at 23 cm and 173 cm above the base of the testing box.
3. The weight of soil required for each 15 cm (6 inch) thickness of the fill was calculated and put into the box. Initially a vibratory compactor (Figure 5.1a) was used to compact the soil, but, as it could not compact the soil to required density, a jackhammer (Figure 5.1b) with a steel plate at the base was used to compact the soil.
4. The first layer of soil nails were installed on top of the first 15 cm (6 inch) compacted soil layer (Figure 5.2). The soil nails were connected to the anchor with the chain links at the endpoint of the nails as shown in Figure 5.3.
5. The soil was compacted in layers with 15 cm (6 inch) lifts for each layer. The second (top) layer of soil nails was installed in the similar manner as the bottom layer.
6. Density tests were conducted after each three layers of compaction for quality control using drive tubes. Compaction tests were conducted in the sample taken with the tubes. Compaction was monitored two times: after compacting the first 0.60 m (24 inch) depth of soil and after 1.05 m (41 inch). The moisture content and density of the compacted soil at these depths were 28.2% and 91.2 lb/ft^3 (1.462 g/cm^3) and 27.1% and 93.4 lb/ft^3 (1.497 g/cm^3), respectively. These values correspond to 92.8% and 95% compaction.

7. The completed soil face before installation of the geotextile and the wire mesh is shown in Figure 5.4 and the details are shown in Figure 5.5.
8. Strain gages were fixed on the soil nails of all four nails on the upper side of the steel rod.
9. Wire mesh was installed as the facing and fixed with the GI spike plates. The connection of the wire mesh and the spike plates is shown in Figures 4.9 and 5.7.
10. After the final layer of soil was compacted the soil was covered with geosynthetic drainage layer with the permeable side down.
11. A water-filled bladder was placed on top of the drainage layer to distribute the surcharge load.
12. A steel plate (Figure 5.7) was placed on top of the bladder.
13. The bladder was punctured at an applied pressure of approximately 4 psi, so the bladder was replaced by geofoam.
14. A vertical load was applied from the top using MTS loading system.
15. Horizontal displacement at the facing was measured by string potentiometers and direct hand measurement from a reference beam.
16. Strains in the soil nails were measured from the affixed strain gages and recorded on smart dynamic strain recorder (DC-204R).
17. Forensic investigation on the test model was done by excavation the section. Notable failure features such as the breakage of anchor connections, crack lines on the soil surface, settlement of the soil wall and the final horizontal movement of the wall face were measured and recorded.

FIGURE 5.1a
Compaction

FIGURE 5.1b
Compaction

FIGURE 5.2
Soil nails installed

FIGURE 5.3
Soil nail connected to the anchor plate with chain links

FIGURE 5.4
Completed soil wall—the front face

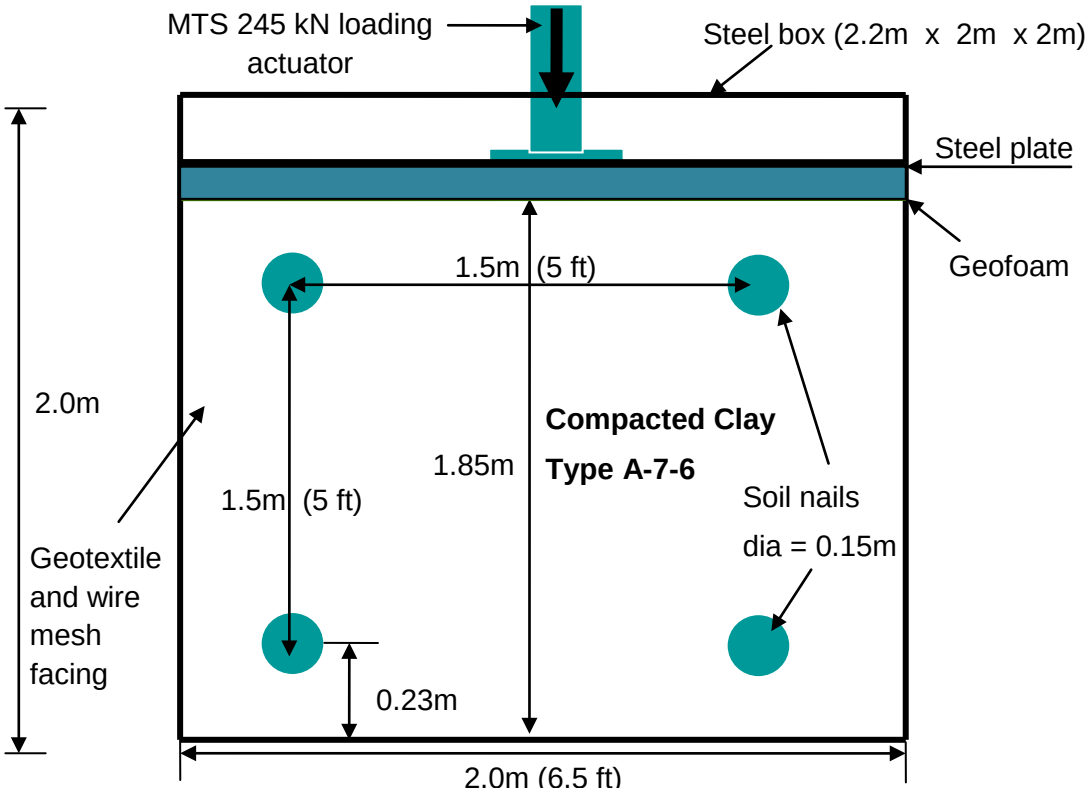

FIGURE 5.5
Front view of the soil nailed wall and the geotechnical box

FIGURE 5.6
String pots on the soil face

FIGURE 5.7
Installing the steel plate on the top of the soil-nailed wall

5.1 Observations

A vertical surcharge was initially applied on the top of soil nailed wall in a series of 2 psi steps. For the initial surcharge of 2 psi, there was no visible change in the majority of the soil face; however, at the soil nail locations, the contact between the wall and the spike plate became tight and the spike plates were holding the wire mesh and the geotextile firmly. At 4 psi, the soil face was pressed slightly out and the maximum deformation was observed at 1 ft above the bottom row of the soil nails. After 4 psi, the load increment was changed to 1 psi. The deformation increased substantially with increased loading and the soil nails failed at the rear nail connections under a 6.7 psi surcharge. The failure occurred with audible sound of something being broken, and the top row of soil nails moved more than 1 ft (31 cm) outward from the initial soil face. Vertical settlement of more than 6 inches (16 cm) at the face was also observed.

Figure 5.8 through Figure 5.13 show the wall face for different surcharges and the final face shape at the time of failure. Figure 5.14 shows the settlement of the soil wall with the application of load on top. The string pot line shown was connected essentially horizontally to

the soil face, but as the soil settled horizontal measurement by string pot became unreliable due to the large amount of vertical settlement of the face as shown in Figure 5.14.

Despite the large deformations, the wire facing and geotextile performed extremely well. No distress of any kind was observed in either material.

Forensic tests showed that at failure, the weld between the chain link and the anchor plates had broken. The 1 cm thick steel anchor had deformed (Figure 5.15) by about 1 inch from the back side of the geotechnical box. Failure of the connection was apparently more due to the downward movement of the nail, which overstressed the chain weld, than pullout stress. Along the width of the box at 1 ft from the back of the wall a 6 inch wide crack developed at failure as shown in Figure 5.16. As the soil nails were pushed out, the anchor plate deformed as shown in Figure 5.17. Other sets of cracking on the top surface along the width of the geotechnical box were observed close to the front face as shown in Figure 5.18. At the time of failure, the soil nails also slid forward by about 15 cm (6 inches) from their original position as seen in Figure 5.15.

Figures 5.19 through 5.21 show the drawings (to scale) of the test setup before the application of any load and after applying 6 psi load.

FIGURE 5.8
Right side of soil face after application of 5 psi surcharge

FIGURE 5.9
Soil face after application of 5 psi surcharge

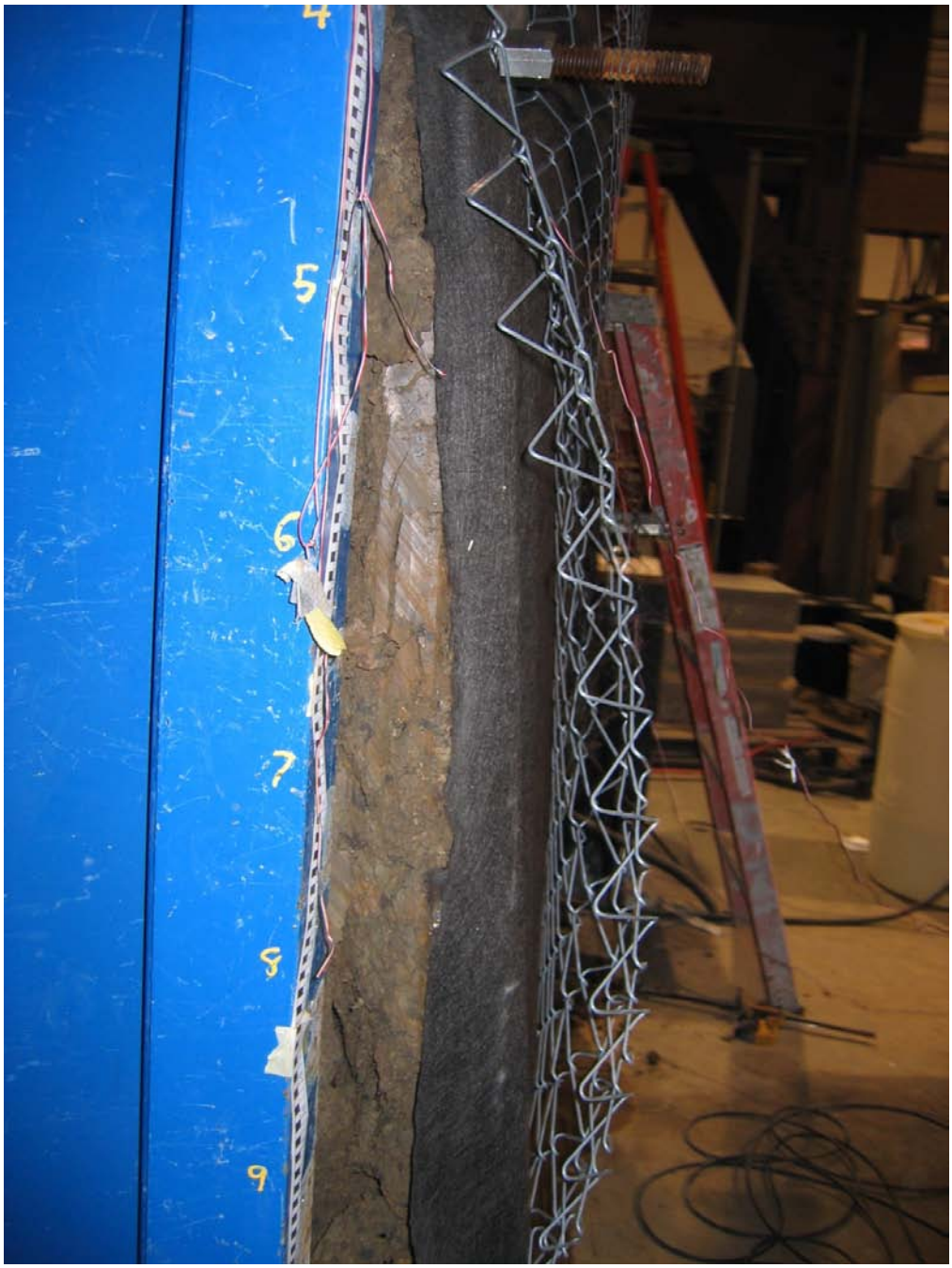

FIGURE 5.10
Soil face after application of 6 psi surcharge

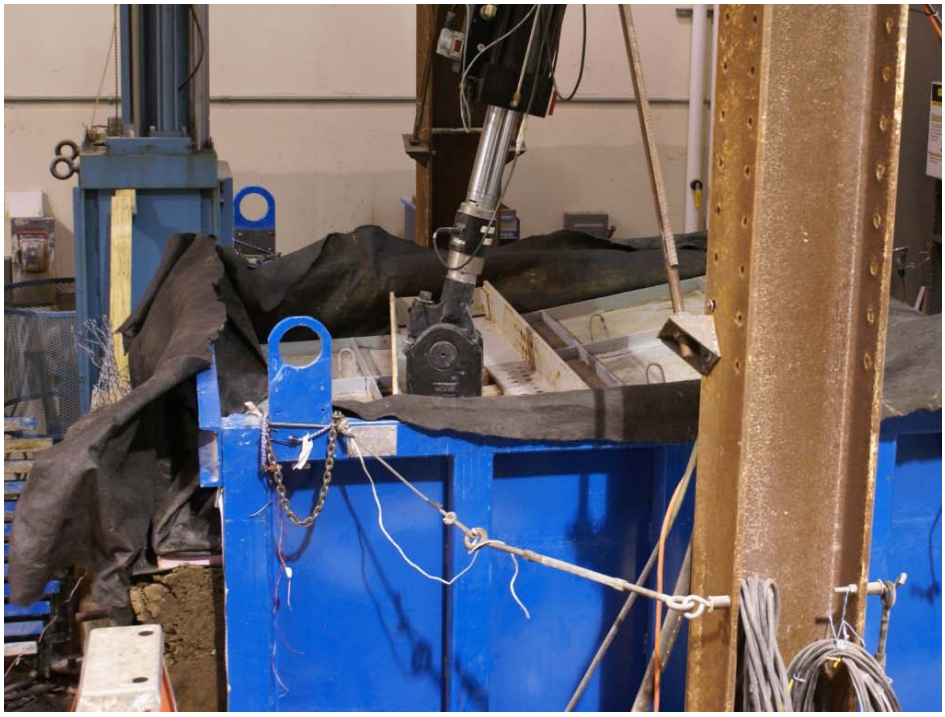

FIGURE 5.11
Side view after failure of nail connections

FIGURE 5.12
Lower left nail after failure

FIGURE 5.13
Side view after failure of nail connections

FIGURE 5.14
Downward movement of string pot connection due to settlement

FIGURE 5.15
Anchor plates pulled out from the rear face of the wall

FIGURE 5.16
Crack developed at failure at 1 ft from the rear face of the wall

FIGURE 5.17
Movement of soil mass out of the rear face of the wall

FIGURE 5.18
Crack seen on the top surface close to the front face of the nailed wall

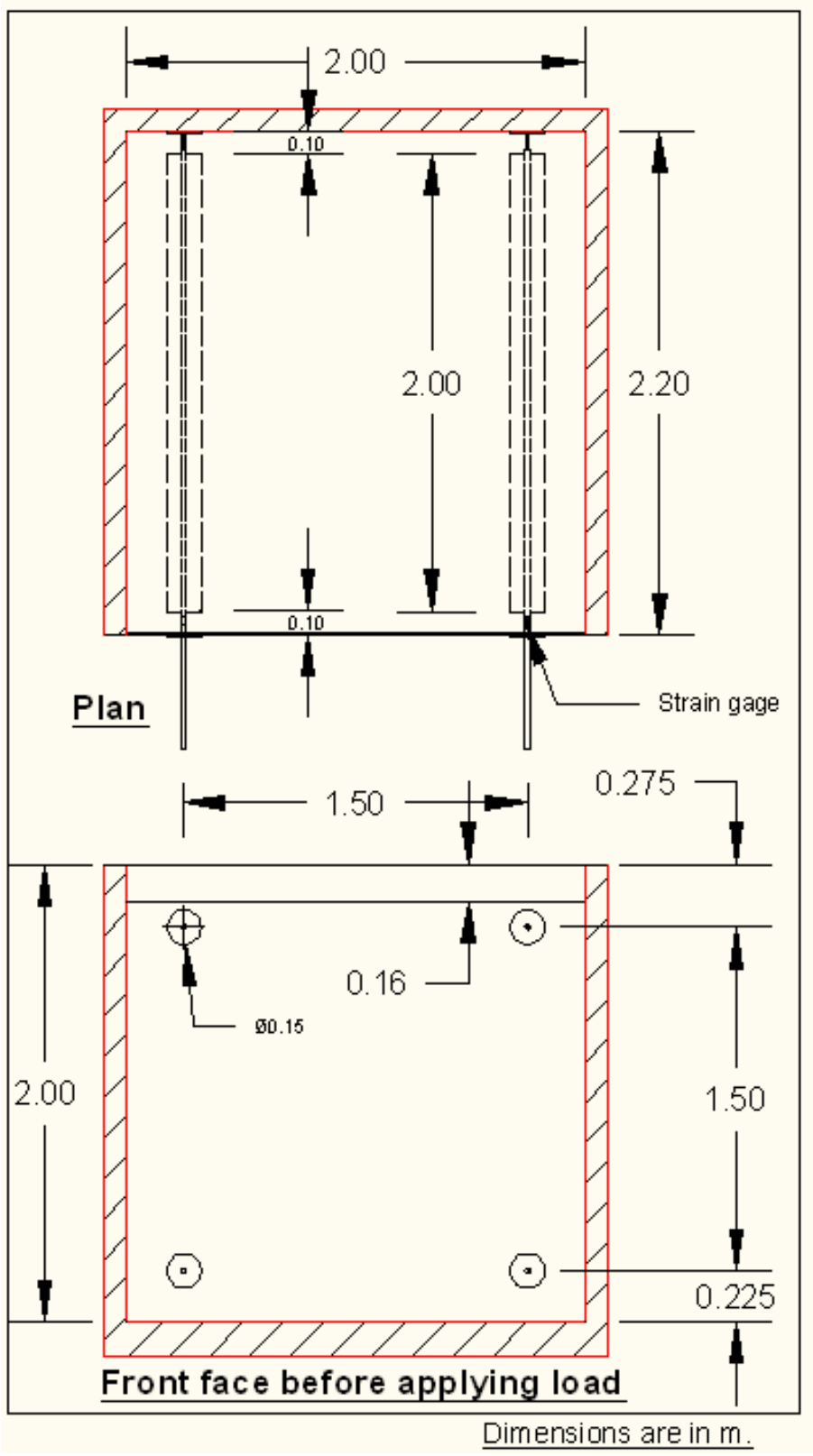

FIGURE 5.19
Position of soil nails at the front face in elevation before test

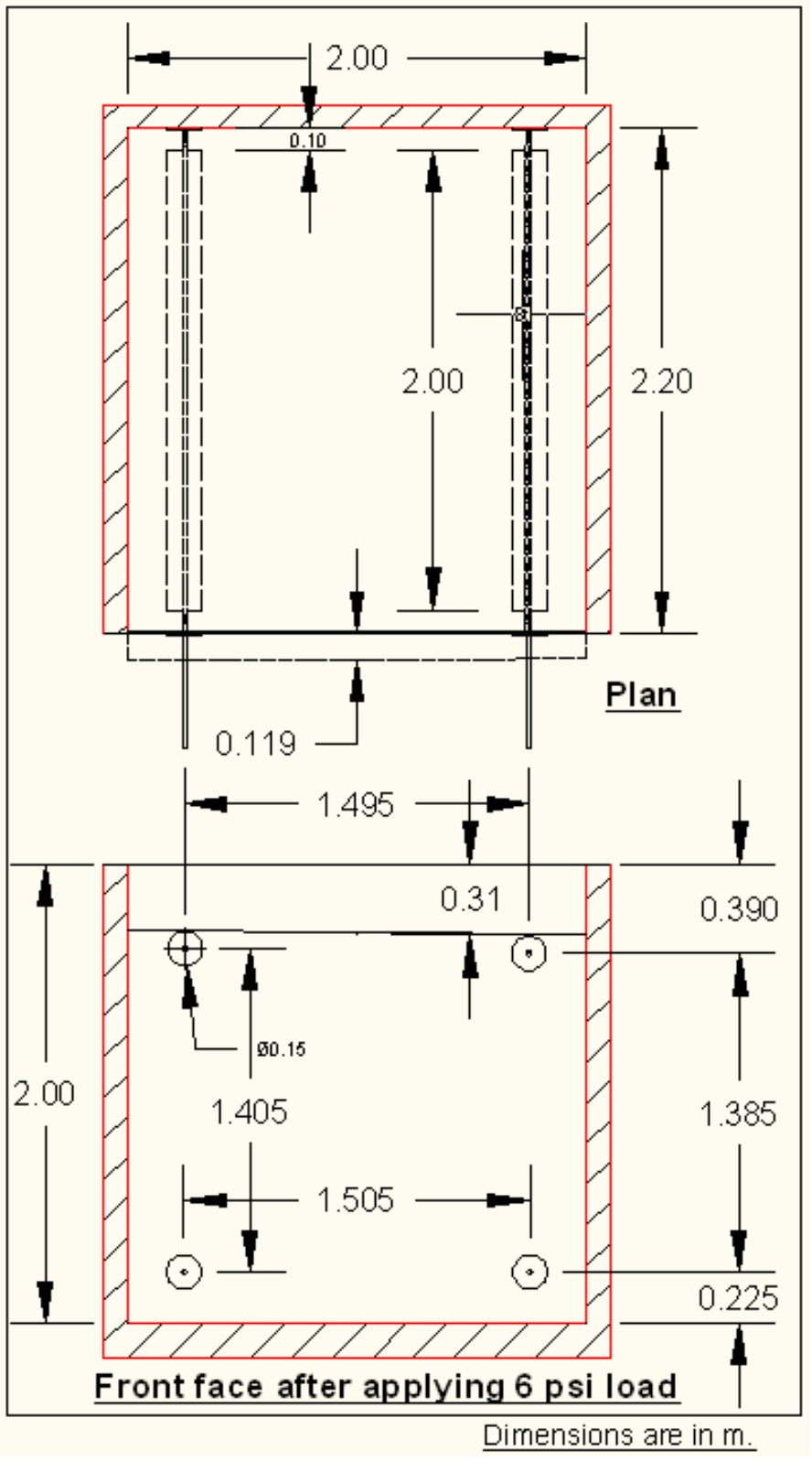

FIGURE 5.20
Position of soil nails at the front face in elevation after application of 6 psi surcharge on top

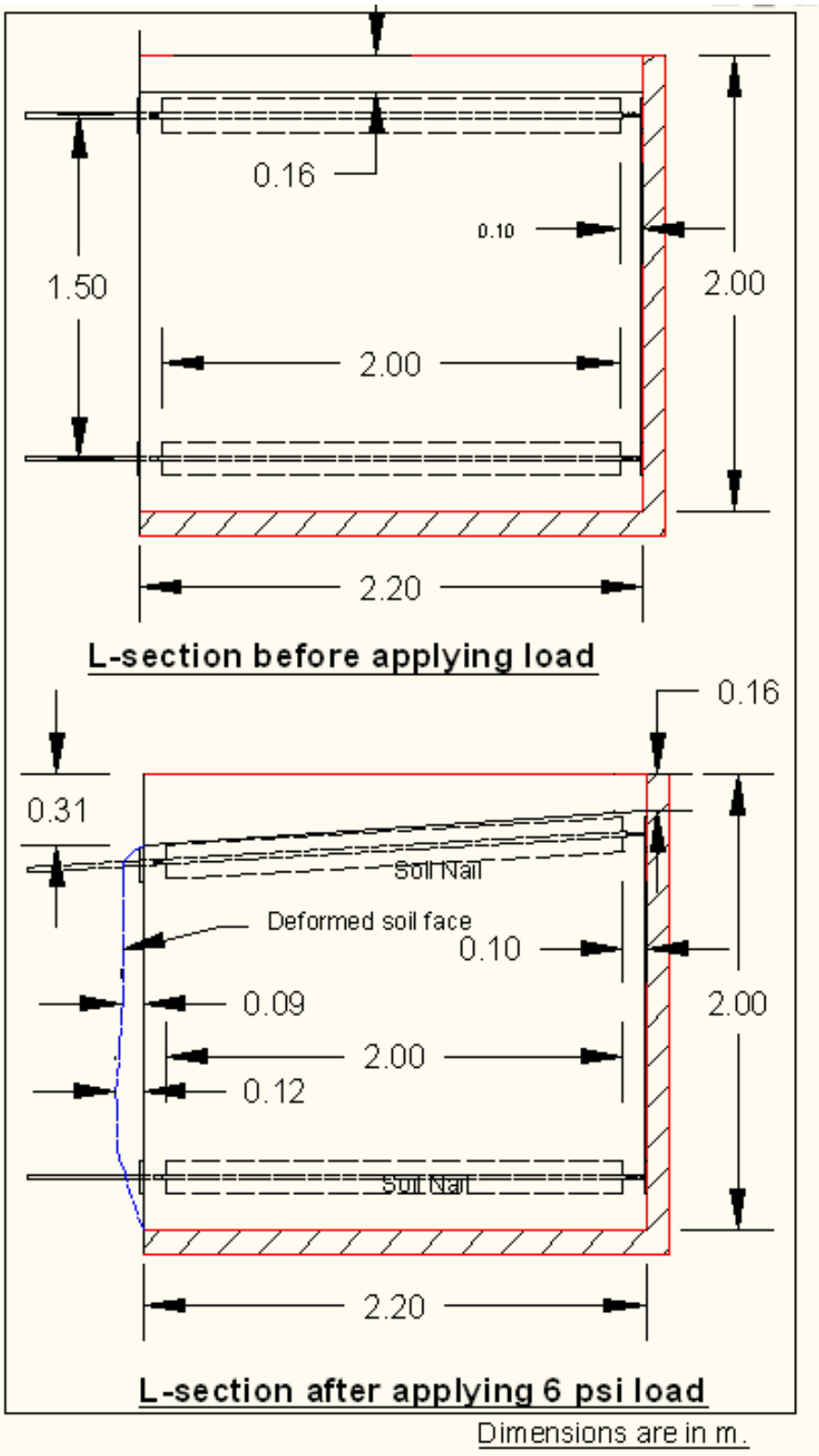

FIGURE 5.21
L-section before applying the load and after applying 6 psi surcharge

Figures 5.22 through 5.24 show how the soil face lead to progressive failure after the application of different load increments at the top.

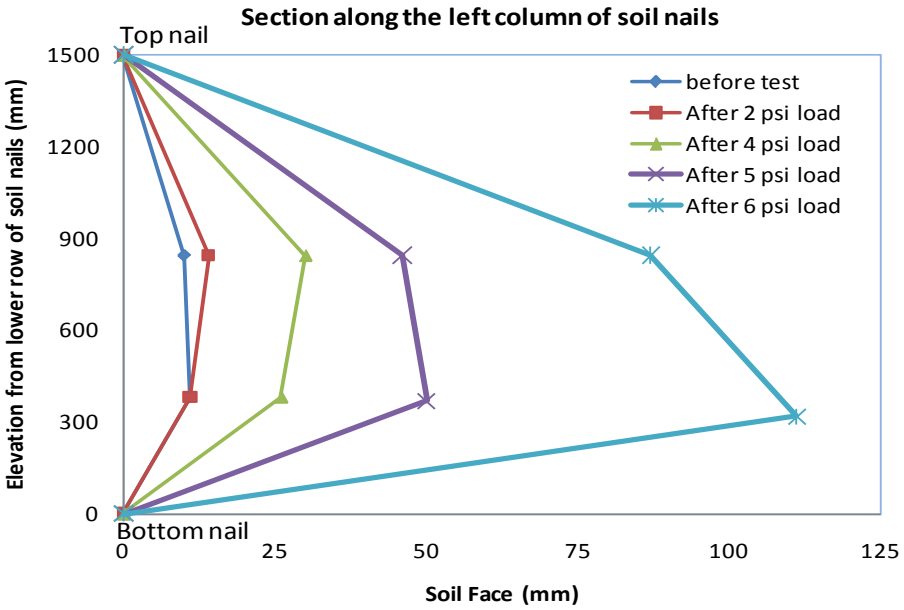

FIGURE 5.22
Position of soil facing along the left column of soil nails after application of different surcharges on top

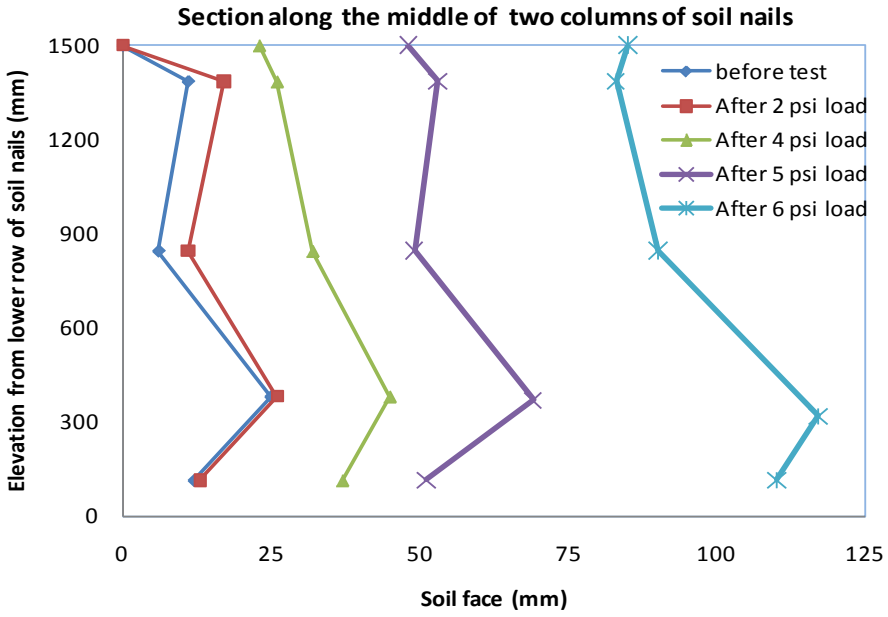

FIGURE 5.23
Position of soil facing midway between the two columns of soil nails with increasing vertical surcharge

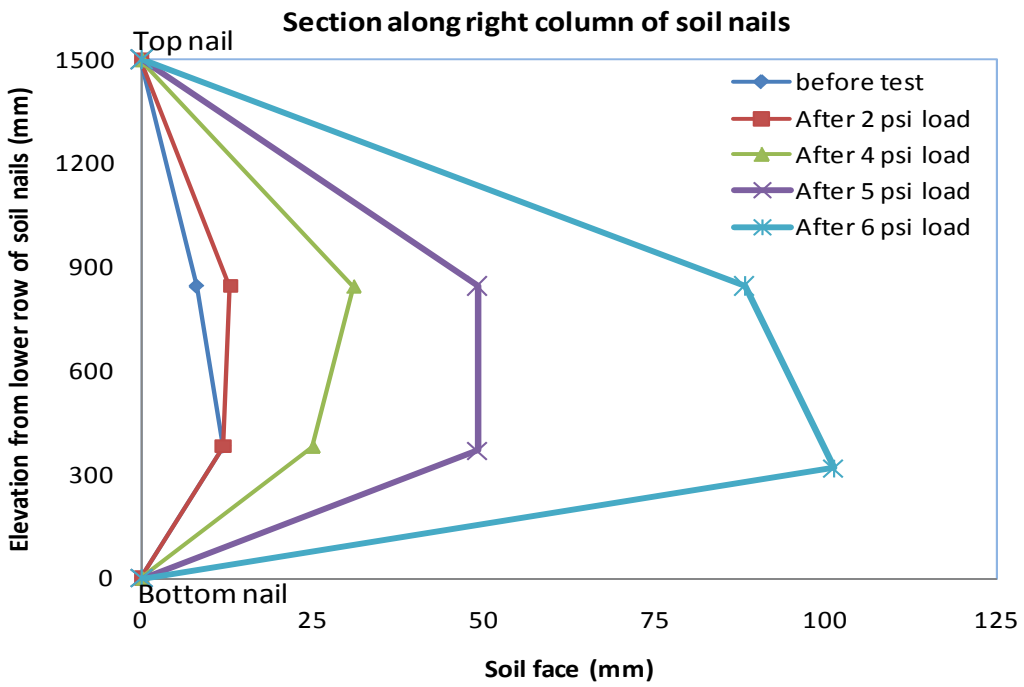

FIGURE 5.24
Position of soil facing along the right column of soil nails with increasing vertical surcharge

The strain gages on the tops of the nails showed larger strains when the nails began to yield in bending due to downward movement of the face. The strains shown in Figure 5.25 are more a function of bending stresses than tension in the nails as the load from the slumping face was transferred to the nails. Stresses from bending were much greater in the upper nails where the soil had more freedom to move.

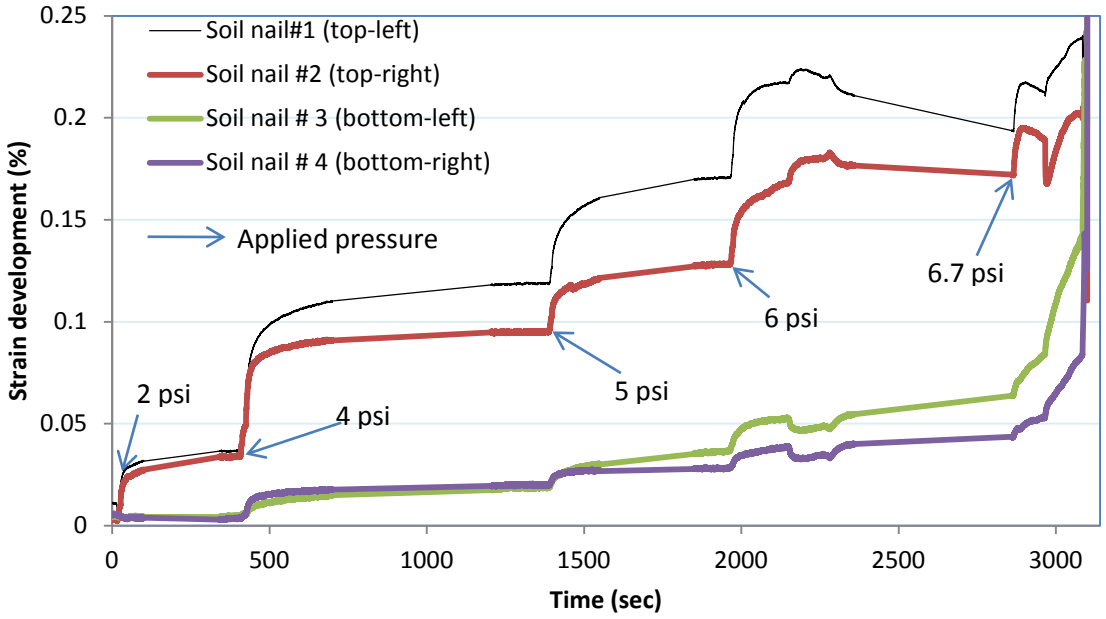

FIGURE 5.25
Strain development at the soil nails at different pressure application on the top of soil nailed wall

5.2 Comments

The soil nails held the face firmly throughout the test. Significant horizontal deformations of the soil face were observed near the bottom of the box and midway between the two columns of soil nails. By this time, the upper row of soil nails had moved slightly outward as the chain link connection between the back of the soil nail and the anchor plate stretched tightly and eventually the anchor plate bent outward as shown in Figure 5.15. At failure, the connection with the anchor plate was broken and the soil nails moved at least 15 cm (6 inch) outward. This phenomenon was not observed in the lower row of soil nails. The major cause of failure of top row of soil nails was the excessive settlement of the soil at top. The vertical deformation of the soil mass caused the upper soil nails to move downward, which transferred a substantial vertical force to the connecting chain link (which broke at 6.7 psi surcharge) and bent the soil nails on top row. Therefore, the vertical deformation (settlement) was more responsible than the horizontal force for the nail failure. Once the upper soil nails failed, the lower rows of nails started to take more load, which can be seen in Figure 5.25, with the increase in strain at approximately 2800 seconds.

These observations are similar to those from the finite difference modeling under long-term loading conditions. Deformations for both the model and physical test were significant for a 5 psi surcharge, with the results for both showing additional settlement between the nails, bulging between the nails, and some crumpling/sagging behavior in the space between the upper nails as can be seen by comparing the results shown in Figures 3.2, 3.4, and 5.21. Minor differences include the location and magnitude of the bulging, which in the physical test tended to be at a lower position between the nails, and more concentrated bulging around the plates. In addition, there was more lateral displacement on the sides of the physical test because the facing was not fixed to the side of the box as it was in the model.

A limitation inherent to the use of the flexible facing method is illustrated in Figure 5.26. In this figure, a 2-dimensional model of a flexible facing shows that the angle α must be greater than zero for there to be a soil retention force transmitted by the facing. For very small angles, the tension in the facing must be very large to develop a significant retention force. Therefore, to develop a significant retentive force, one or more of the following conditions must occur:

1. The flexible facing is installed against a slope with $\alpha \approx 0$. Significant movement of the soil is required to engage the facing.

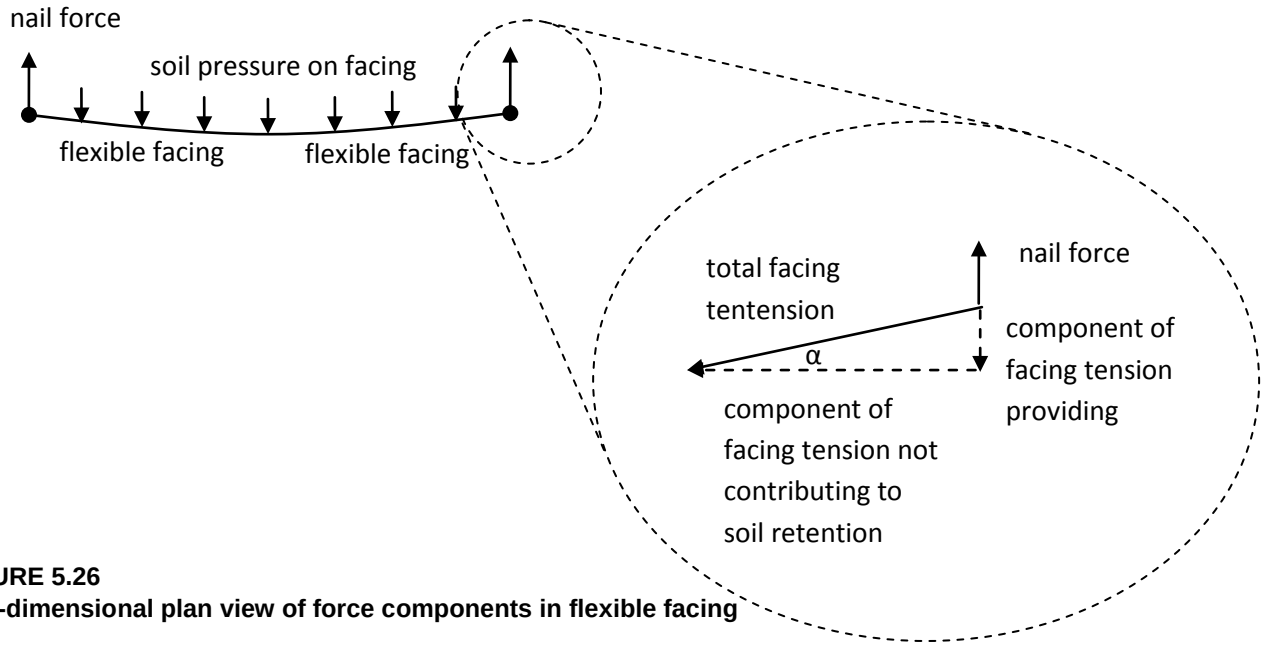

FIGURE 5.26
Two-dimensional plan view of force components in flexible facing

2. The facing is pretensioned mechanically. Some movement is still required to engage the facing, but not as much as without pretensioning.
3. Short, intermediate nails are placed between the primary nails. By reducing the horizontal span, α will increase to a significant angle with much less horizontal movement.
4. "Shape" the wall face prior to installation of the facing so that $\alpha > 0$ before installation. This could be done by removing additional soil from around the nail holes and not completely filling the holes with grout prior to attachment of the facing (see Figure 5.27). In this way, the facing could be pretensioned and α made greater than zero by tightening down the base plates.

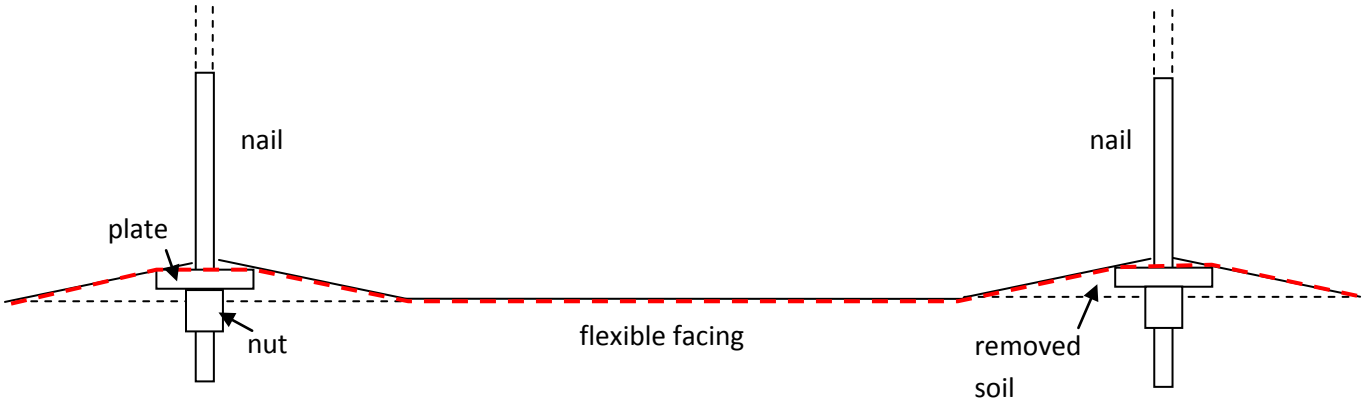

FIGURE 5.27
Plan view of face "shaping" concept to have α > 0 and facing tension > 0 at installation

Chapter 6: Conclusions and Recommendations

The following conclusions and recommendations were developed based on the finite difference modeling and the physical testing described in this report.

Finite difference modeling was effective in predicting the behavior of the soil in the physical test. Specifically, the shape and relative magnitude of the deformations and the approximate load at which deformations would become very large were relatively accurate and provided useful guidance in designing the physical test.

The wire mesh and the geotextile did not appear to be overstressed at any point during the testing, and in this aspect, they performed very well. However, both the finite difference modeling and the physical testing provide strong evidence that soil nail walls with flexible facing in clay with high plasticity could result in large deformations of the face and significant settlements at the surface, even for walls that are relatively short. A major reason for this is that significant deformation is required to mobilize the tensile strength of the facing. Although the facing was stretched as tightly as possible by hand before testing, the soil face still had to move outward significantly before the wire mesh provided significant lateral confinement to the face. Mobilization of the mesh at a smaller lateral deformation is possible but would require at least machine stretching of the facing material, and may require “shaping” of the wall face with nail connections recessed into the slope. A face shaped in this way would cause the membrane tension to increase when the nuts were tightened on the soil nails, and confinement would be applied to a degree upon installation. These actions would require additional contractor effort and quality control.

Based on these results, it is recommended that use of soil nail walls with flexible facing in clay be limited to short walls where significant deformations are tolerable or to conditions that are not as demanding, such as steep slopes or in higher quality soils.

References

Alston, C. and R. E. Crowe. 1993. Design and construction of two low retaining wall systems restrained by soil nails anchors. *Transportation Research Record* 1414: 49–58.

Byrne, R.J., D. Cotton, J. Porterfield, C. Wolschlag, and G. Ueblacker. 1998. *Manual for design and construction monitoring of soil nail walls.* Report FHWA-SA-96-069R. Washington, D.C.: Federal Highway Administration.

Geobrugg. 2007. Soil nailing and anchoring a temporary shoring application. Slope stabilization system/technical documentation.

Plumelle, C., F. Schlosser, P. Delage, and G. Knochenmus. 1990. French national research project on soil nailing: Clouterre. *Geotechnical Special Publication No. 25*:660–675.

Wong, I. H., B. K Low, P. Y. Pang, and G. V. R. Raju. 1997. Field performance of nailed wall in residual soils. *Journal of Performance of Constructed Facilities* 11 (3):105–112.

Yuan, J. X., Y. Yang, L. G. Tham, P. K. K. Lee, and Y. Tsui. 2003. New approach to limit equilibrium and reliability analysis of soil nailed walls. *International Journal of Geomechanics* 3 (2):145–151.

K-TRAN

KANSAS TRANSPORTATION RESEARCH AND NEW-DEVELOPMENT PROGRAM

AD ASTRA PER ASPERA

Kansas

Department of Transportation